LBL-27366 c.2

Lawrence Berkeley Laboratory
UNIVERSITY OF CALIFORNIA

CHEMICAL BIODYNAMICS DIVISION

RECEIVED
LAWRENCE
BERKELEY LABORATORY

FEB 8 1990

LIBRARY AND
DOCUMENTS SECTION

To be published as a chapter in **Manganese Redox Enzymes**, V.L. Pecoraro, Ed., VCH Publishers, New York, NY

The Photosynthetic Water Oxidation Complex Studied by EPR and X-Ray Absorption Spectroscopy

K. Sauer, V.K. Yachandra, R.D. Britt, and M.P. Klein

May 1989

TWO-WEEK LOAN COPY

This is a Library Circulating Copy which may be borrowed for two weeks.

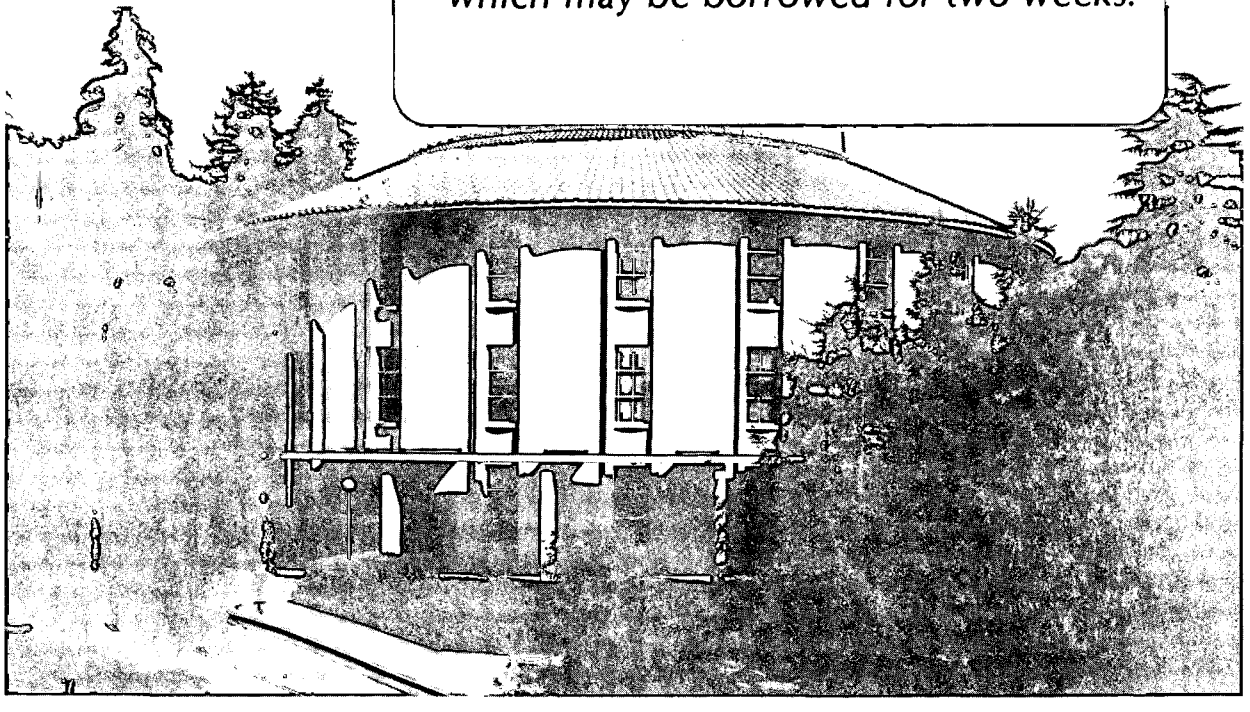

LBL-27366 c.2

Prepared for the U.S. Department of Energy under Contract Number DE-AC03-76SF00098.

DISCLAIMER

This document was prepared as an account of work sponsored by the United States Government. While this document is believed to contain correct information, neither the United States Government nor any agency thereof, nor the Regents of the University of California, nor any of their employees, makes any warranty, express or implied, or assumes any legal responsibility for the accuracy, completeness, or usefulness of any information, apparatus, product, or process disclosed, or represents that its use would not infringe privately owned rights. Reference herein to any specific commercial product, process, or service by its trade name, trademark, manufacturer, or otherwise, does not necessarily constitute or imply its endorsement, recommendation, or favoring by the United States Government or any agency thereof, or the Regents of the University of California. The views and opinions of authors expressed herein do not necessarily state or reflect those of the United States Government or any agency thereof or the Regents of the University of California.

Manganese Redox Enzymes, V.L. Pecoraro, Ed.
VCH Publishers, New York

The Photosynthetic Water Oxidation Complex Studied by EPR and X-ray Absorption Spectroscopy

Kenneth Sauer,[#] Vittal K. Yachandra, R. David Britt and Melvin P. Klein

Department of Chemistry[#] and Chemical Biodynamics Division
Lawrence Berkeley Laboratory, University of California
Berkeley, CA 94720

Introduction

One of the central questions related to the photosynthetic oxidation of water to molecular oxygen has been the mechanism by which four electrons are removed from two water molecules to produce an O_2 molecule by the reaction

$$2\,H_2O \Longrightarrow O_2 + 4\,H^+ + 4\,e^-$$

The photosynthetic reaction centers, which provide the energy that drives photosynthetic water oxidation, give every evidence of transferring electrons one at a time. Measurements of the yield of oxygen released by a train of saturating light flashes by Joliot and by Kok and their coworkers around 1969-70 showed a clear periodicity of four.[1] The results provided definitive evidence for the involvement of a complex that stores oxidizing equivalents so as to release O_2 only after four equivalents have been accumulated.

The essential involvement of manganese in water oxidation was foreshadowed by the observation by Pirson in 1937 that plants or algae[2] deprived of Mn in their growth medium lost the ability to evolve O_2. Addition of this essential element to the growth medium resulted in a restoration of water oxidation within 30 min. Once procedures for isolating chloroplasts and, subsequently, Photosystem II (PS II) enriched O_2-evolving membrane fragments were established, more direct evidence for the involvement of manganese was obtained. For example, several treatments were devised which appeared to inhibit electron transfer reactions between PS II and the water oxidation complex. The Tris-washing inhibition, explored in detail by Yamashita and Butler,[3] was found not only to be reversible[4] but also to involve the release and subsequent re-uptake of Mn in the process.[5]

The stoichiometry of Mn per oxygen-evolving complex has been somewhat controversial, although the majority of workers in the field now favor a value of 4 Mn / PS II reaction center.[6] Problems in defining this number precisely arise from several sources. Manganese is present in excess in the chloroplast cytoplasm (stroma), and a variety of loose binding sites cause it to be carried along in thylakoid membrane preparations. Most of this loosely bound Mn can be removed by treatment with chelating agents like EDTA, but the latter serve also to extract other divalent ions like Ca^{2+} that play a catalytic role in some of the steps in electron transfer associated with water

oxidation. On the other hand, the tightly bound Mn with the stoichiometry of about 4 per reaction center are not all equivalent, as measured by their release by the various inhibitory treatments.[6] There has been more than one study claiming that not all of these Mn are essential for active oxygen evolution. While the jury may still be out on this question at the time of this writing, we will support the majority view in this article.

The S-state cyclic mechanism proposed by Kok and coworkers[1b] in 1970 was originally formulated as follows

$$S_0 \xrightarrow{h\nu} S_1^{1+} \xrightarrow{h\nu} S_2^{2+} \xrightarrow{h\nu} S_3^{3+} \xrightarrow{h\nu} S_4^{4+} \longrightarrow S_0 + O_2$$

Each successive photon activation of the reaction center causes the transfer of one electron from the catalyst S until four equivalents are accumulated. At that point the catalyst spontaneously releases O_2 from water and reverts to the most reduced state, S_0. This mechanism has had an enormous influence on thinking related to the understanding of photosynthetic water oxidation. Although it did not specify particular chemical intermediates or the stage where water molecules were taken up, the mechanism did provide a rationale for most of the experiments that measured the pattern of O_2 release and subsequently, when appropriate measurements were made, also for the pattern of release of protons.[7] In studies of the role of Mn in this process workers have generally adopted the Kok model and have attempted to characterize the oxidation state and structural parameters of the individual S-states. In this regard it is significant to note that the resting state (dark-adapted) is not the most reduced state, S_0, but one that is one step more oxidized, designated S_1. Upon subsequent illumination, the complex proceeds in a regular fashion through the states S_2 and S_3 (each of which can be trapped at low temperature, for example), through the hypothetical state S_4, which is unstable with respect to O_2 release, returning to S_0, whereupon further illumination restores it to S_1. In practice the process is not quite so clean as indicated above, for a small fraction (10%) of photon absorptions lead to misses that fail to advance the cycle and another fraction (5%) advance the cycle by two steps The mechanisms for these processes are not understood, but they result in a fairly rapid dephasing of the system during a prolonged train (25) of flashes. Several recent reviews have comprehensively covered the previous literature on photosynthetic water oxidation.[8]

During the first decade following the introduction of the Kok model little information appeared concerning the role of Mn in the advance of the S-states, largely because of the absence of suitable spectroscopic signals. During the past ten years this situation has changed significantly, owing largely to the discovery and characterization of EPR and X-ray absorption spectra associated with Mn in particular S-states. Because these spectra can be related directly to the contribution of Mn, they have been especially valuable in proving for the first time that Mn changes its oxidation state along with the S-state advance. The next sections will summarize the contributions in this area from EPR and X-ray absorption studies.

Electron Paramagnetic Resonance Detection of Manganese

EPR Studies of the Role of Manganese in Photosynthetic Water Oxidation. Dismukes and Siderer[9] published the first report of an EPR signal attributable to a multinuclear Mn center in Photosystem II. Their EPR experiments were performed on dark-adapted broken spinach chloroplasts which were subjected to a series of light flashes and then quickly frozen. A single flash was seen to produce a broad low-temperature "multiline" EPR signal with at least sixteen partially resolved hyperfine lines with a regular interpeak separation of about 80 G. This multiline structure was interpreted as resulting from magnetic interactions between 2 Mn in a binuclear complex, or possibly among 4 Mn in a tetranuclear complex.[9,10] The multiline EPR signal amplitude was diminished by a second, third, or fourth flash, increased following a fifth flash, and diminished again after a sixth flash. The amplitude vs. flash dependence was thus seen to follow the period-four dependence of the Kok S-state cycle. The dark-adapted chloroplasts were poised primarily in the S_1 state. The multiline EPR signal exhibited maximal amplitude after the first and fifth flashes, and the signal was thus assigned to the S_2 state of the Kok water oxidation cycle. Brudvig *et al.*[11] demonstrated that the multiline EPR signal could be generated by continuous illumination at cryogenic temperatures. The kinetics of the formation and decay of the multiline signal were consistent with the S_2 state assignment, and the maximal generation of the signal by continuous illumination occurred at a temperature of about 190 K. Figure 1a displays the multiline EPR spectrum generated in PSII-enriched membranes from spinach poised in the S_2 state by 195 K illumination.

The pattern of partially resolved hyperfine lines observed for this multiline EPR signal is similar to that observed in the EPR spectra of binuclear mixed-valence Mn compounds.[12] For example, di-μ-oxo bridged Mn(III)-Mn(IV) complexes give rise to EPR signals with 16 well-

resolved lines with a regular spacing of about 80 G (Fig 2). These 16 lines result from the superposition of 36 nearly isotropic lines expected from hyperfine coupling to the 2 non-equivalent ^{55}Mn nuclei, each with nuclear spin I=5/2. The oxygen bridges mediate a strong antiferromagnetic exchange interaction between the S=3/2 Mn(IV) ion and the high-spin S=2 Mn(III) ion. The EPR-visible ground state of the antiferromagnetically coupled system exhibits an effective spin S=1/2. The resulting Mn hyperfine couplings measured in the EPR spectrum are determinined by the projections of the isolated Mn ion hyperfine couplings upon this effective spin S=1/2 state that results from the vector coupling of the isolated ion electronic spins. For a Mn(III)-Mn(IV) system, the two effective hyperfine couplings are $A_1 = 2 \cdot A(\mathrm{Mn(III)})$ and $A_2 = -1 \cdot A(\mathrm{Mn(IV)})$, where A(Mn(III)) and A(Mn(IV)) are the hyperfine couplings for the isolated Mn ions. In the limit where $A(\mathrm{Mn(III)}) \approx A(\mathrm{Mn(IV)})$, the magnitudes of the two effective hyperfine couplings A_1 and A_2 are in the ratio of 2:1, resulting in a degeneracy of many of the 36 hyperfine lines and giving rise to the observed 16 line spectrum. Antiferromagnetically coupled Mn(II)-Mn(III) systems also can produce "multiline" EPR signals.[13] The effective hyperfine couplings for a Mn(II)-Mn(III) system are $A_1 = 7/3 \cdot A(\mathrm{Mn(II)})$ and $A_2 = -4/3 \cdot A(\mathrm{Mn(III)})$.[9] However from measurements of the Mn X-ray absorption edge energies in PS II-enriched membranes (see next section), we prefer a Mn(III)-Mn(IV) assignment to a Mn(II)-Mn(III) origin of the multiline EPR signal that arises from the S_2-state. The S_2 EPR signal from PS II preparations typically exhibits 19 partially resolved hyperfine lines rather than the 16 lines measured from the di-μ-oxo bridged Mn(III)Mn(IV) complexes. This difference may result simply from greater anisotropy in the g-tensor of the PS II Mn complex.

We have previously noted that there are at best estimate 4 Mn ions per PS II reaction center. However, the S_2 multiline EPR signal closely resembles EPR signals observed from compounds with only 2 magnetically coupled Mn ions. If more than 2 Mn ions are present in a complex, with each ion contributing a large hyperfine coupling to the net electron spin, we anticipate the occurrence of EPR transitions over a broader magnetic field range than is actually observed.[14] However, it is possible that 4 Mn ions contribute to the EPR lineshape, but that the major hyperfine features result from only 2 of the 4 ions. Such a situation could arise from a tetranuclear Mn complex with oxidation states Mn(IV)•3Mn(III). A limiting case of such a tetranuclear complex would consist of a pair of antiferromagnetically coupled binuclear complexes, with a weak magnetic interaction between the two binuclear complexes. In the limiting case of vanishing magnetic coupling between the two binuclear complexes, a Mn(III)-Mn(IV) pair gives rise to the multiline signal, and the S=0 ground state of a Mn(III)-Mn(III) pair is EPR silent. The presence of non-zero coupling between the pairs will introduce a "transferred hyperfine interaction", resulting

in a small hyperfine contribution from the diamagnetic Mn(III)-Mn(III) complex. More general exchange coupling schemes can also give rise to similarly small contributions from 2 of the 4 Mn ions in a tetranuclear complex with oxidation states of either Mn(IV)•3Mn(III) or Mn(III)•3Mn(IV).[15] The magnitude of these couplings may be too small to generate resolvable splittings using conventional EPR spectroscopy. We note that the resolution of the major Mn hyperfine lines that compose the S_2 multiline signal is poor compared to the EPR spectra of mixed valence model compounds. This is not necessarily due to extra inhomogeneous broadening associated with the biological environment. For example, the multiline EPR signal arising from the binuclear Mn active site of a Mn-containing catalase shows resolution comparable to that obtained with model compounds.[16] The S_2 multiline EPR signal shows some additional structure superimposed upon the major partially resolved Mn hyperfine peaks.[17] It is possible that the substructure observed on the PS II S_2 multiline signal and the broad widths of the major lines result from small hyperfine contributions from an additional two Mn ions. Four Mn ions would contribute a total of 1296 lines to the signal, and only the largest couplings would be resolved. However this is at best weak evidence for a tetramer. For example, addition of relatively small g-tensor anisotropy would reduce the apparent resolution of the EPR spectrum from that of a binuclear center and would increase the number of peaks in a field-modulated EPR spectrum. Hyperfine anisotropy may also increase the complexity of the EPR spectrum from that of a binuclear center. We therefore consider the observed S_2 Mn EPR signal to provide definitive proof of a Mn cluster of at least two ions. However the data provided by this signal alone do not clearly distinguish between a binuclear, tetranuclear or possibly trinuclear Mn cluster.

Casey and Sauer[18a] and Zimmermann and Rutherford[18b] demonstrated the formation of another light-induced EPR signal in PS II-enriched membranes. This EPR signal is centered at a magnetic field corresponding to g=4.1 (Fig 1b). The linewidth of the light-induced g=4.1 signal is about 320 G, and it presents no resolved hyperfine structure. Casey and Sauer formed this g=4.1 EPR signal via continuous illumination of PS II-enriched membranes at a temperature of 140 K. Subsequent warming of 140 K-illuminated samples to 190 K results in the disappearance of the g=4.1 signal along with the appearance of the multiline Mn signal. Zimmermann and Rutherford observed the g=4.1 signal in PS II membrane preparations illuminated at 200 K in the presence of sucrose, which apparently stabilizes this EPR signal at these higher temperatures. In a later paper, Zimmermann and Rutherford[19] presented the results of examining the magnitude of this g=4.1 EPR signal as a function of flash number in a fashion similar to the original Dismukes and Siderer experiment[9] on the multiline EPR signal. They concluded that the g=4.1 signal also

arises from the S_2 state. Cole *et al.*[20] demonstrated a shift of the Mn X-ray K-edge to higher energies for PS II membranes illuminated at 140 K and exhibiting large light-induced g=4.1 EPR signals. The Mn X-ray edge shift for these samples is comparable to that observed with 190 K illumination and the production of the Mn multiline EPR signal. This observation suggests that the g=4.1 EPR signal also results from oxidation of Mn on the $S_1 \rightarrow S_2$ transition. Although the multiline EPR signal is observed in PS II-enriched preparations from cyanobacteria,[21] to date they have yielded no g=4.1 EPR signals.[21b] EPR signals with effective g-values of approximately 4 may be observed in S=3/2 spin systems. A $g \approx 4$ component dominates the EPR spectrum for a disordered S=3/2 spin system with an axial zero-field splitting if the magnitude of the zero-field splitting $2D$ is larger than the Zeeman splitting term $g\beta H$.[22] Mn(IV) in an octahedral environment has a net electron spin S=3/2, and broad $g \approx 4$ EPR signals have been observed in mononuclear Mn(IV) model complexes.[23] Furthermore, $g \approx 4$ EPR signals observed in these Mn(IV) complexes do not always show resolved Mn hyperfine couplings, so the lack of observed Mn hyperfine structure on the PS II g=4.1 signal does not preclude a Mn ion origin for this signal. Hansson *et al*[14] have therefore proposed that the S_2 g=4.1 signal arises from an isolated Mn(IV) ion in an axially distorted octahedral environment, and that this mononuclear Mn site is in redox equilibrium with a binuclear Mn site that gives rise to the multiline S_2 EPR signal. Another model for the origin of the g=4.1 signal was proposed by de Paula *et al.*[15b] They suggested that the g=4.1 EPR signal arises from an EPR-observable S=3/2 substate of an exchange-coupled tetranuclear Mn complex. In their model, the multiline S_2 EPR signal arises from an S=1/2 substate present in a different conformation of the tetranuclear Mn center. Such a spin-state interconversion is known to exist in Fe-S clusters. For example, the $[4Fe\text{-}4S]^{+1}$ cluster of the Av2 protein of *Azotobacter vinelandii* nitrogenase is present in two interconvertible forms, one with a ground state S=1/2 and the other with a ground state S=3/2.[24]

In summary, EPR studies have demonstrated that the oxygen-evolving complex of Photosystem II contains a multinuclear Mn complex. The miminum number of ions forming the EPR-detectable complex is two. However, the results from EPR spectroscopy have not provided an unambiguous assignment of the exact geometry of the complex, or even the number of Mn ions which form the complex. Two possible assignments are (1) a tetranuclear Mn complex with two conformations which give rise to either the multiline or g=4.1 EPR signals in the S_2 state, and (2) a binuclear Mn complex which produces the multiline EPR signal and is in redox equilibrium with at least one of the two remaining Mn ions, with this isolated ion giving rise to the g=4.1 EPR signal upon oxidation to Mn(IV). Details of these two models for the origin of the two S_2 EPR signals,

as well as their dependence on factors such as illumination conditions, presence of oxygen-evolution cofactors and inhibitors, and the use of various cryoprotectants, will be presented in other chapters of this volume.

Electron Spin Echo Envelope Modulation Studies of the Role of Manganese in Photosynthetic Water Oxidation. Hyperfine couplings between unpaired electron spins in Mn *d*-orbitals and the I=5/2 spins of two ^{55}Mn nuclei give rise to the major features of the S_2 multiline EPR signal. The isotropic components of the Mn hyperfine interactions are due to the polarization of electrons in the 1*s*, 2*s*, and 3*s* shells by exchange interactions with the unpaired *d* electrons. This "core polarization" gives rise to Mn hyperfine interactions with magnitudes on the order of 80 G. These large splittings are observed in the S_2 multiline EPR signal as approximately 19 partially resolved EPR lines. There will also be magnetic interactions with any paramagnetic nuclei present as ligands to the Mn complex. These "superhyperfine" interactions will be much weaker than the Mn self-hyperfine interactions that are partially resolved in the EPR spectrum. In fact, these superhyperfine interactions are too weak to result in resolved splittings even in mixed-valence Mn model compounds with much narrower EPR linewidths. An example is provided by the EPR spectrum of the di-μ-oxo bridged Mn(III)-Mn(IV) compound with 2,2'-bipyridine terminal ligands. Figure 2 displays the EPR spectrum of this complex prepared with the nuclear spin I=1/2 ^{15}N isotope incorporated into the 2,2'-bipyridine ligands. There are no resolved ^{15}N superhyperfine couplings observed in this spectrum, even though the Mn hyperfine lines are narrow and the I=1/2 ^{15}N nitrogen isotope provides superhyperfine couplings 40% greater than the naturally abundant I=1 ^{14}N isotope.

In general, we expect relatively small values for ligand superhyperfine couplings in high valence Mn compounds with nearly octahedral ligand coordination. The d^3 Mn(IV) ion exists in the $t_{2g}^3 e_g^0$ electronic state. The singly occupied d_{xz}, d_{xy}, and d_{yz} orbitals project away from the coordinating ligands, so the overlap of the unpaired spin density onto the ligand orbitals will be small. The high-spin d^4 Mn(III) ion exists in the $t_{2g}^3 e_g^1$ electronic state. In this case, one of the two e_g orbitals is occupied by an unpaired electron, and this orbital will project onto a set of the coordinated ligands. However, the d^4 Mn (III) ion is subject to a large Jahn-Teller distortion which weakens the overlap of the singly occupied e_g orbital and the ligand orbitals, again resulting in relatively small superhyperfine coupling. The weak superhyperfine couplings expected for these ions can be contrasted to the strong superhyperfine couplings observed for ions such as square-

planar d^9 Cu(II), which has a large overlap between the unpaired spin in the $d_{x^2-y^2}$ orbital and the four square-planar ligands.[25] Because ligand superhyperfine couplings are not resolved even in mixed-valence Mn model compounds, we do not expect to observe superhyperfine couplings for the much broader lines present in the PS II S_2 multiline EPR signal. In addition, no information about electric quadrupolar couplings for spin $I > 1/2$ ligand nuclei will be contained in the conventional EPR spectra. However, the information that would be gained if such superhyperfine and electric quadrupolar couplings could be measured is enormous, because one could determine these couplings for a variety of paramagnetic nuclei in protein ligands, inorganic cofactors, and substrate and inhibitor molecules. To obtain such information, we have introduced pulsed EPR methods to the study of the oxygen-evolving Mn complex of Photosystem II.

In a conventional EPR experiment, a small fraction of the continuously applied microwave radiation is absorbed by those electron spins in resonance. The incident microwave power is typically kept sufficiently low to avoid saturation of the electron spin populations. The spin system is therefore maintained nearly at thermal equilibrium. Pulsed EPR is performed in a different manner, with powerful microwave pulses effecting large rotations of the net electron spin magnetization on a timescale short compared to the relaxation processes which return the electron spin magnetization to equilibrium. For very narrow EPR signals, the EPR spectrum can be obtained by Fourier analysis of the Free Induction Decay (FID) following a single microwave pulse. However, the large bandwidths of most EPR signals, in particular those associated with transition metals, preclude such simple pulsed EPR experiments. In such cases only a small fraction of an inhomogeneously broadened EPR line is excited by the microwave pulse. The FID may reflect only the excitation profile of the incident pulse and often decays to undetectable power levels before the instrument receiver recovers from the pulses. However, the rapid dephasing due to inhomogeneous broadening may be refocussed with multiple pulse sequences, resulting in one or more observable electron spin echoes. In addition to inducing the electron spin transitions, the microwave pulses may also induce "semi-forbidden" transitions of paramagnetic nuclear moments magnetically coupled to the electron spins, resulting in quantum mechanical coherences in the nuclear spin sublevels associated with the electron spin levels. These coherences create interference effects which can be measured by varying the electron spin echo pulse timings. Fourier analysis of the resulting Electron Spin Echo Envelope Modulation (ESEEM) pattern reveals the frequencies of the various nuclear transitions. These frequencies can then be interpreted to determine superhyperfine and electric quadrupolar couplings. The ESEEM technique is most useful for examining relatively weak couplings. Nuclear transitions with frequencies much larger

than the excitation bandwidth of the applied microwave pulse (about 25 MHz in our instrument) will not be observed. The ESEEM technique is thus complementary to ENDOR spectroscopy, which works best for nuclei with large hyperfine or superhyperfine couplings. Details of experimental and theoretical aspects of the use of the ESEEM technique are provided in several good review articles.[26]

The ESEEM technique has been employed to study nitrogen ligation to high-valence Mn in the di-μ-oxo bridged Mn(III)-Mn(IV) compound with either the ^{15}N or ^{14}N isotopes of nitrogen incorporated into the 2,2'-bipyridine terminal ligands.[27] The electron spin echo envelopes obtained with these complexes are deeply modulated by interactions with either the ^{14}N or ^{15}N nitrogen isotopes. The frequencies and amplitudes of these modulation components have been examined at a number of field positions across the broad EPR spectra . The observed modulation can be attributed to a class of nitrogen ligands with superhyperfine couplings of $A(^{14}N)$~2.8 MHz or $A(^{15}N)$~4.0 MHz. Such a small coupling would correspond to a line splitting of only 1 G in the EPR spectrum for a single coordinated ^{14}N ligand; and, as noted above, no resolved nitrogen couplings are observed via conventional EPR of this complex, even though the Mn hyperfine lines show much better resolution than those in the PS II Mn multiline EPR signal.

Our ESEEM study investigating the mechanism of ammonia inhibition of oxygen evolution provides an excellent example of the utility of this pulsed EPR technique for studying the PS II Mn complex.[28] Amines have long been known to inhibit photosynthetic oxygen evolution. Sandusky and Yocum described two independent sites for amine inhibition of oxygen evolution.[29] One site shows inhibition by a number of amines, and this inhibition is competitive with respect to Cl^- concentration. A second site shows inhibition independent of Cl^- concentration; ammonia inhibits oxygen evolution at this site, but alkyl amines do not. Beck *et al* [30] later demonstrated that ammonia treatments in the presence of high Cl^- concentration causes an alteration of the S_2 Mn multiline EPR signal. This result indicates that ammonia binding to the Cl^--independent inhibition site affects the magnetic properties of the Mn complex. However, no differences were observed between the altered multiline EPR signals generated with $^{14}NH_4Cl$ and $^{15}NH_4Cl$ treatments, and thus there was no experimental evidence for non-zero nitrogen superhyperfine couplings, a requirement for conclusively assigning the effect to direct coordination of ammonia to the Mn complex. Without evidence of nitrogen superhyperfine coupling, there is the possibility that the alteration of the multiline EPR signal arises indirectly upon binding of ammonia elsewhere in the complex than as a Mn ligand. Such behavior is observed[31] with the similar alteration of the Mn

multiline signal by replacement of the essential oxygen evolution cofactor Ca^{2+} by Sr^{2+}. Our ESEEM experiments provide definitive evidence that an ammonia-derived ligand binds directly to the Mn complex.[28] We prepared samples of PS II-enriched membranes treated with either $^{14}NH_4Cl$ or $^{15}NH_4Cl$ at a concentration (100mM, pH=7.5) sufficient to inhibit oxygen evolution. ESEEM spectra of the Mn multiline signal recorded following low-temperature illumination (195 K) are identical for control, $^{15}NH_4Cl$-treated, and $^{14}NH_4Cl$-treated samples. However, the ESEEM results obtained after a brief warming of these samples to 20 °C show dramatic differences between the three samples. (Fig 3a,b,c) The $^{15}NH_4Cl$-treated sample shows a new feature which arises from an I=1/2 ^{15}N nucleus with an isotropic component of the superhyperfine coupling of $A(^{15}N)$=3.22 MHz. The $^{14}NH_4Cl$-treated sample shows a different spectrum, with features arising from an I=1 ^{14}N nucleus with $A(^{14}N)$=2.29 MHz, a value that scales to the measured ^{15}N superhyperfine coupling by the ratio of the magnetic moments of the two nitrogen isotopes. The magnitude of the superhyperfine coupling is similar to that of the nitrogen ligands provided by 2,2'-bipyridine in the di-μ-oxo bridged Mn(III)-Mn(IV) complex, and we consider this to be strong evidence that the ammonia-derived species is directly coordinated to the PS II Mn cluster. The nitrogen binding observed via ESEEM occurs during the "annealing" step, indicating that ammonia binds at the S_2 state of the Kok cycle, but not at the cryogenic illumination temperature (195 K). In this sense, the ligand binding is correlated with the formation of the altered Mn multiline signal.[30]

The I=1 ^{14} N nucleus has a non-zero electric quadrupole moment which interacts with the electric field gradients produced by the chemical bonds to the nitrogen atom. The electric quadrupolar terms can be effectively isolated by performing the ESEEM experiment at a point in the EPR spectrum such that the externally applied magnetic field cancels the superhyperfine field produced by the electron. In this case the ESEEM experiment measures the ^{14}N "zero-field splittings" which arise solely from the electric quadrupole interaction. These low-frequency transitions are best observed using a three-pulse ESEEM scheme, as in Fig 3d. This figure displays the three "zero-field" transitions from the ammonia-derived ^{14}N ligand to the Mn complex. The electric quadrupole parameters for this ^{14}N ligand are e^2qQ=1.61 MHz and η=0.59, where e^2qQ is a measure of maximum amplitude of the electric field gradient, and the asymmetry parameter η describes the degree of axial symmetry of the bonding environment, ranging from η=0 for perfect axial symmetry to η=1 for maximal rhombic symmetry. The measured value of η=0.59 indicates a deviation from axial symmetry greater than expected for a metal-coordinated NH_3 ligand. We have advanced a model for ammonia inhibition where the oxidation of Mn that

occurs during the $S_1 \rightarrow S_2$ transition triggers a deprotonation of a transiently bound NH_3, forming a NH_2 bridge between Mn and another hard metal cation, at the same time blocking a water binding site.[28]

We have shown that the ESEEM technique can provide detailed information about superhyperfine and electric quadrupolar couplings that are far too small to be observed with conventional EPR methods. For example, the 400 kHz frequency of the lowest ^{14}N ESEEM transition in the ammonia-binding experiment is approximately 1/100 the magnitude of the smallest splittings resolved in the conventional EPR spectrum. We are currently applying the ESEEM technique to determine the ligand environment of the Mn cluster and to study potential substrate binding using different paramagnetic nuclear isotopes in water.

X-Ray Spectroscopy of Manganese

X-ray absorption spectroscopy (XAS) is element specific and, hence, is a good method for studying the structure of Mn in the O_2-evolving complex without interference from the pigment molecules, the lipid and protein matrix, or other metals like Ca, Mg, Cu or Fe which are present in active PS II preparations.[32] Mn X-ray K-edge spectra provide information about oxidation states and site symmetry of the Mn complex, and Mn Extended X-ray Absorption Fine Structure (EXAFS) furnishes information about the numbers, types and distances to neighboring ligand atoms.[33] Few other spectroscopic techniques provide such specificity for studying the structure of Mn in the O_2-evolving complex in the photosynthetic apparatus. The preparations that we have used for the X-ray absorption experiments, from either spinach or the cyanobacterium *Synechococcus*, contain several peptides, pigment chlorophyll molecules, and electron transfer components of Photosystem II.[34] The preparations are fully functional in terms of O_2 evolution and can be poised in the various S-states from S_0^* to S_3.

Mn K-edge Spectra of the Oxygen Evolving Complex. The K-edge inflection energy of a first row transition element reflects principally the 1s-4p transition energy in an isolated atom.[35] However, in a metal complex containing ligands bonded to the metal, the assignment of the principal K-edge region and the near edge region becomes very complicated and as yet there is no satisfactory theoretical methodology available.[36] Presumably the principal transition is from the 1s level of the metal to a molecular orbital with some p-character. The position of the K-edge depends

on the nature of the ligands, and in general the metal atom with more electron-donating ligands is characterized by a lower inflection point energy. It has also been shown that the K-edge inflection energy shifts to higher values upon increasing the oxidation state of the metal.[37] These correlations permit an approximate oxidation state assignment for the metal when the nature of the ligands is known, or when it is known that there is no change in ligands; a shift to higher energy results from an increase in the oxidation state of the metal complex. Despite the necessary reservations some important conclusions can be reached from X-ray edge studies.

The oxidation state of the Mn complex in the O_2-evolving complex increases upon advancement from the S_1 to the S_2 state. This conclusion is based on a shift in the inflection point energy from ~6551 to ~6552 eV for spinach.[20,38,39] A similar shift to higher energy in the inflection point energy is observed in *Synechococcus*, but the inflection point energies of both the S_1 and S_2 states are about 0.5 eV lower than those for the corresponding states in spinach.[21b] Samples in the S_2 state in spinach or *Synechococcus* were prepared by illumination at 190 K or by illumination at 277 K in the presence of DCMU; these are protocols that limit the PS II reaction center to one advance. Both methods produce an S_2 state characterized by the presence of the EPR multiline signal . An alternative protocol involving illumination at 140 K results in an EPR signal at g=4.1 in spinach. A g=4.1 EPR signal is not observed in *Synechococcus*, however. Each of these protocols for spinach or *Synechococcus* increases the edge inflection energy by about 1 eV.[21b,38,39]

In mononuclear Mn inorganic complexes the K-edge inflection point energy shifts by about 2 eV on average for a one-electron oxidation.[37a] Assuming that four Mn are present per PS II, we proposed earlier[20,21b,38,39] that the S_1 to S_2 edge shift of 1 eV is what one expects from a one- or two-electron oxidation of the Mn complex. Recent XAS data from multinuclear Mn complexes show that the nuclearity of the Mn complex has a significant effect on the shift in the Mn K-edge inflection point energies for a one-electron oxidation.[40] For example, in bi, tri and tetranuclear Mn complexes with the same or similar ligands and coordination environment but with oxidation states differing by one equivalent, the shift in the edge inflection energy can range from 1 to 2 eV. The edge inflection energies of a representative set of bi-, tri- and tetranuclear Mn complexes in similar coordination environments but different oxidation states are presented in Table Ia. It is known from EPR and EXAFS studies that the Mn in the O_2-evolving complex is present as a multinuclear complex, and a comparison of the magnitude of the edge shift in PS II to those from multinuclear

complexes suggests that a one-electron oxidation of the Mn complex is more likely for the S_1 to S_2 transition.

It can be argued that structural changes and not oxidation state changes are responsible for the K-edge energy shift observed in PS II samples in the S_1 to S_2 transition. We find that significant structural rearrangements would be required to produce edge shifts of the magnitude seen in PS II. A comparison of multinuclear complexes in similar oxidation states but with different coordination environments shows that the inflection point energy is sensitive to the bridging structure (Table Ib), but is relatively insensitive to changes in the terminal ligands. As shown in Table Ib, the K-edge inflection point shifts by 0.4 to 0.6 eV on replacing a di-μ_2-oxo bridge by a mono-μ_2-oxo and μ_2-acetate bridges, with no change in the oxidation state of the complex. Such changes in the bridging ligands invariably result in an increase in the Mn - Mn distance from 2.7 Å to greater than 3 Å, as discussed in the next section. Because we do not observe evidence in the EXAFS spectra for any such structural changes in the S_1 to S_2 transition, we conclude that the edge shift of about 1 eV corresponds to a change of one oxidation equivalent associated directly with the Mn.

A similar shift of 1 eV, but to lower energy, is observed on going from S_1 to an S_0-like state, denoted S_0^*, which can be induced by incubation with NH_2OH followed by illumination. The lower Mn K-edge energy of S_0^*, relative to the edge of S_1, implies the storage of an oxidative equivalent within the Mn cluster during the S_0 to S_1 transition; however, this has not yet been confirmed by measurements directly on the normal S_0 state.[41]

The Mn K-edge inflection point of preparations poised in the S_3 state (65% S_3, achieved by a low temperature illumination under conditions that resulted in a double turnover of a dark-adapted PS II preparation) is the same as that for the S_2 state. This formation of S_3 is accompanied by the loss of the EPR multiline signal. Thus, the oxidative equivalent stored within the O_2-evolving complex during this transition may reside on another intermediate donor to the Mn complex or on one of its ligands. It is also possible that the lack of an edge shift in the S_2 to S_3 transition is a consequence of partial oxidation of water which results in no change in the effective oxidation state of Mn.[42]

Simulations of the EPR multiline signal have shown that the Mn is in a mixed-valence complex involving Mn(II,III) or Mn(III,IV),[9,10,15a] but it is not possible to decide between these alternatives on the basis of EPR. From a comparison of the Mn K-edge inflection energy of a series of Mn complexes with PS II preparations we conclude that Mn atoms in the O_2-evolving complex in the S_2 state are predominantly in the (III) and (IV) oxidation states. We therefore assign the oxidation state of the S_2 state as either (III,III,III,IV) or (III,IV,IV,IV). Different possibilities (a-d) for oxidation state changes during the S_0^* to S_3 transitions are presented in Table II. We shall consider the possibilities that are based on the above assignments for the S_2 state together with the K-edge results that indicate that there is a one-electron oxidation of the Mn complex during each of the S_0 to S_1 and S_1 to S_2 transitions, but with no furhter oxidation during the S_2 to S_3 transition.

The pre-edge region, in which semi-allowed 1s-3d transitions are present, also yields information about the oxidation state. These transitions are formally forbidden by dipole selection rules and generally become "allowed" by mixing with 4p orbitals. The structure of the pre-edge region of the Mn K-edge transitions is systematically different in Mn(III) and Mn(IV) model complexes. These differences in the edge spectra are presumably related to systematic symmetry differences between Mn(III) and Mn(IV) complexes which in turn give rise to differences in the energies of the d electron levels and/or differences in matrix elements for 1s-3d transitions. The pre-edge region of the K-edge spectra of S_1 samples resemble those of many Mn(III) complexes, while for S_2 samples this region of the spectrum resembles those of Mn(IV) complexes. These results are strongly suggestive that in the S_1 to S_2 transition a Mn(III) atom is oxidized to Mn(IV).[43] Similar conclusions about oxidation state changes of the Mn complex for the S_1 to S_2 transition were proposed using optical absorbance difference spectroscopy,[44] and NMR and EPR relaxation measurements.[45]

The EXAFS measurements on the S_1 and S_2 states have failed to detect any change in the structure of the Mn complex during this transition.[39] Such invariance of the EXAFS spectrum is not consistent with an oxidation of Mn(II) to Mn(III) as has been shown in a study of multinuclear Mn complexes. The heterogeneity in Mn-Mn and Mn-ligand atom distances in systems containing both Mn(II) and Mn(III,IV) leads to destructive interference in the EXAFS wave. The decreased intensity observed for the Fourier peaks in the radial distribution plot is beyond any reasonable contribution from the Debye-Waller factor. In contrast the EXAFS spectrum of multinuclear

complexes is quite insensitive to Mn oxidation state changes from (III) to (IV). Based on the K-edge and EXAFS results we assign the oxidation state of the S_1 state as (III,III,III,III) or (III,III,IV,IV), which rules out scheme d in Table II.

The K-edge results show that the oxidation state decreases by one equivalent on going to the S_0^* state from the S_1 state. The EXAFS results show that there is a significant change in the structure of the complex during the S_0^* to S_1 transition.[41] By comparison to inorganic model compounds we have shown that this structural change is consistent with oxidation of Mn(II) to Mn(III) in a multinuclear complex (see below). These results lead to an assignment of (II,III,III,III) or (II,III,IV,IV) for the oxidation state of the Mn complex in the S_0^* state, which leaves schemes a and b as the likely models for the oxidation state changes during the S_0^* to S_3 state transitions. This assignment is consistent with results from NMR and EPR relaxation measurements.[44,45] Despite earlier disagreement between two different groups[44] concerning the interpretation of optical absorbance difference spectroscopy results, a consensus has now been achieved in assigning the S_0 to S_1 transition to the oxidation of Mn(II) to Mn(III).[46]

As shown above, the results from the Mn K-edge studies are in agreement with the conclusions derived from optical absorbance studies, NMR and EPR relaxation results for the S_0, S_1 and S_2 states.[44-46] However, the optical studies are indicative that there is also oxidation of Mn(III) to Mn(IV) during the S_2 to S_3 transition, which is at variance with the Mn K-edge data and the NMR and EPR relaxation data. At present we do not understand the discrepancy in the results between the methods. It has been argued from studies with multinuclear Mn model compounds that optical difference spectra alone cannot be used with confidence to distiguish Mn(II) to Mn(III) from Mn(III) to Mn(IV) oxidation state changes.[47] X-ray edge studies also cannot be used to assign the oxidation state of metals in every case. For example, in Fe-S clusters where there is significant delocalization onto the S ligand atoms, oxidation or reduction of the clusters does not produce a significant edge shift.[48] Nevertheless, in the case of Mn complexes with N or O ligands we do not find a *single instance* among the many sets of compounds with similar ligands and coordination environment that we have examined[40b] where a change in oxidation state of Mn is not accompanied by a K-edge shift.

The Mn K-edge spectra are quite similar in spinach and *Synechococcus* preparations.[21b,39] The similarity of the edge structure and of the multiline signal in spinach and *Synechococcus* are suggestive that the oxidation states are the same for the two organisms. The edge energy for *Synechococcus* is smaller (0.5±0.3 eV) compared with that for spinach; this may owe to small differences in the Mn complex, such as differences in the ligands, or ligand environment of Mn in the two organisms.

Summarizing the Mn K-edge data, the evidence supports a change in oxidation state of Mn in the S_0^* to S_1 to S_2 transitions. There is no apparent change in the oxidation state of the Mn during the S_2 to S_3 transition. This does not exclude the possibility that the oxidizing equivalent is stored on a ligand of Mn. Redox active ligands for Mn have been proposed previously.[49] The most likely schemes for oxidation state changes in the S_0^* to S_3 states are a and b in Table II.

EXAFS studies of Mn in the Oxygen Evolving Complex. EXAFS data provide a composite measure of the coordination of all the Mn atoms in the system. Despite this limitation EXAFS analysis has provided important insights into the structure of the Mn complex in the O_2-evolving complex and the changes that the Mn complex undergoes on advancement from the S_0^* through the S_3 states.

Mn EXAFS data from PS II samples are fit by the Teo-Lee method, which uses theoretical values for the backscattering amplitude and phase shifts induced by the absorber-scatterer atom pairs.[50] The average distance and the number of scattering atoms from Mn are obtained by a nonlinear least-squares fitting program. We have used this method of EXAFS analysis for simulating the data from crystallographically characterized multinuclear Mn complexes, and this method of analysis successfully simulates the oxo-bridging Mn - O distances, the Mn - O or N terminal ligand distances, and the Mn - Mn distances for these complexes. The Fourier transforms of EXAFS data of PS II samples in the S_1, S_2 and S_3 states are shown in Fig. 4. The first Fourier peak is best simulated by two shells of O or N ligands, and the second Fourier peak at higher R is best simulated by scattering from a single shell of Mn.

The salient features from our EXAFS studies of the S_1 and S_2 states from spinach and *Synechococcus* are as follows: 1) *There are 1 to 2 N or O ligand atoms at about 1.8 Å.* The range of uncertainty in this number is ± 0.05 Å. Typically, uncertainties in distances from EXAFS

are between ± 0.015 and ± 0.03 Å. However, the EXAFS oscillations due to scattering from ligand atoms at short distances are convolved with the background and this increases the error limits. We have verified the presence of the feature at about 1.8 Å for both spinach and *Synechococcus* preparations by using two different methods of detection. Each of these experiments involves an entirely different background contribution. The 1.8 Å feature is a necessary component of the simulations of data from every sample.* Furthermore, bridging Mn-O distances are typically about 1.8 Å in multinuclear μ_2 or μ_3 oxo-bridged Mn complexes.[52-54]

- - - - - - - - - - - - - -

Footnote

*It is incorrectly suggested by George *et al* [51] that the discrepancy between their data and ours with regard to the presence of a 1.75 - 1.8 Å Mn-O component is due to the theoretical functions for phase shift and amplitudes employed in our analysis and to background subtraction problems. The fitting routine employed in our analysis correctly simulates the bridging distances of about 1.8 Å and the number of bridging ligands in more than 20 different inorganic complexes that we have studied.[40b] As indicated in the text, we have shown that the presence of the 1.8 Å distance in the simulations is not correlated with the background contribution. Some causes for the discrepancy in these results are indicated later in this chapter.

- - - - - - - - - - - - -End of Footnote- - - - - - - - - - - - -

2) *There are 2 to 4 N or O ligand atoms at 1.9 - 2.2 Å.* We find this range of distances in all of our samples, and it reflects the presence of a distribution of bond lengths in the Mn complex. It is difficult to determine the number of scatterers when there is such a spread of distances. Comparison to multinuclear Mn complexes shows that such a large distribution of distances is typical of Mn-O or N terminal ligand distances.[52-54] 3) *On average each Mn atom has 1 - 1.5 Mn atom neighbors at a distance of about 2.7 Å.* Similar results have been obtained from spinach and the thermophilic cyanobacterium *Synechococcus* .[21b,39,41,42]

The coordination numbers and bond lengths derived from the EXAFS data closely resemble the crystal structure parameters from oxo-bridged Mn (III) and (IV) complexes. Examination of a series of multinuclear Mn complexes reveals that the Mn-Mn distances range between 2.6 - 2.8 Å in complexes where two Mn atoms are bridged by at least two μ_2-oxo,[52] or two μ_3-oxo bridges.[53] (An additional μ_2-acetate bridge is also present in some of these complexes.) In the complexes that contain the μ_3-oxo bridges there is also a Mn - Mn distance at greater than 3 Å, as illustrated in Fig. 5. The Mn-Mn distance decreases to 2.3 Å when the two Mn atoms are linked by three μ_2-oxo bridges.[52d] In complexes that contain two μ_2-carboxylato

bridges and/or one μ_2-oxo bridge, the Mn-Mn distance is greater than 3 Å,[54] and in some complexes can be as large as 3.5 Å.[53b]

The important point is that there exist *at least two μ-oxo bridges* between pairs of Mn atoms in all reported complexes that have a Mn-Mn distance of about 2.7 Å. Therefore we propose that the Mn complex in the O_2-evolving complex contains minimally a di-μ-oxo bridged structure. This conclusion is principally based on the observation of the 2.7 Å Mn-Mn distance, but it is also supported by the presence of the Mn-O distance at 1.75 - 1.8 Å, which is characteristic of Mn-O^{2-} distance in multinuclear Mn complexes.[52-54]

It is not possible to distinguish between two μ_2-oxo or two μ_3-oxo bridges between pairs of Mn atoms based solely on the presence of the 2.7 Å distance; in inorganic complexes both linkages are characterized by 2.6-2.8 Å Mn-Mn distances. However, complexes containing μ_3-oxo linkages between Mn atoms have an additional Mn-Mn distance of >3Å. We do not observe any peaks in the Fourier transforms (Fig. 4) at such distances. Therefore it is more likely that the pairs of Mn atoms are linked by μ_2-oxo bridging ligands. [We previously identified a feature at 3.2 Å, by adding EXAFS data from a PS II sample in the S_1 to those of one in the S_2 state to increase the signal-to-noise.[55] We have been unable to reproduce this feature in data sets from single samples with our current detection system (Fig. 4). We have examined more than 20 different PS II samples using data with a much higher signal-to-noise ratio (*e.g.*, Fig.4) compared to those on which the preliminary report was based.]

The use of a solid state lithium-drifted silicon detector with energy discrimination[56] instead of the plastic scintillator PM tube array[57] which was used in our previous work with PS II preparations, has allowed us to collect EXAFS data that are free from background artifacts and that can be simulated with excellent agreement. The essential conclusions for spinach and *Synechococcus* have remained the same as mentioned above,[21b,39,41,42] but we are able to narrow the range of uncertainty in the number of Mn scatterers at 2.7 Å to between 1 and 1.5, which allows us to discount certain multinuclear structures for the Mn complex as discussed below.

This leads to the question of what are likely structures for the Mn complex in the O_2-evolving complex. We propose minimally a di-μ-oxo bridged structure between two Mn atoms; because there are four Mn per PS II, this implies that there are at least two di-μ-oxo bridged structures present in the complex. Additional carboxylate bridges between the Mn atoms cannot be

discounted. The relative arrangement of the two moieties is at present unknown, and it is a matter of debate and speculation. There are several different ways one can arrange pairs of Mn atoms linked by two μ-oxo bridges and also satisfy the condition that, on average, each Mn sees 1 to 1.5 Mn scatterers at 2.7 Å. The simplest interpretation is that there are two distinct binuclear complexes, with the distance between them greater than 3.0 Å, as illustrated in Fig. 6. An average of one Mn scatterer is seen by each Mn at 2.7 Å in this configuration.

At the same time, we cannot rule out linear or bent trimers or tetramers, or highly distorted cubane-like structures[53c] with each Mn seeing 1 to 1.5 Mn scatterers at 2.7 Å. Linear trimers or tetramers with 2.7 Å Mn-Mn distances have not yet been synthesized, but reports of the synthesis of linear or bent trimers with Mn-Mn distances of 3.4-3.5 Å have appeared.[58] The 1 to 1.5 Mn scatterers observed at 2.7 Å excludes the symmetric cubane proposed by Brudvig *et al*[59] and the 'butterfly' tetranuclear clusters proposed by Christou *et al*[60] as possible candidates for the Mn complex in the OEC. The number of back scatterers at 2.7 Å are 3 and 0.5 (average per Mn) for the symmetric cubane and the 'butterfly' structure, respectively.

Recently, George *et al* [51] have reported EXAFS spectra of the dark-adapted state from spinach using oriented chloroplast membranes. George *et al* reproduced the feature that we reported earlier at 2.7 Å and also the scattering from N or O ligand atoms at 1.89 - 2.27 Å. In addition, peaks at 3.3 and 3.8 Å are reported. The Fourier transforms of their data show distinct peaks which correspond to Mn ligand distances shorter than 1.89 Å. These Fourier peaks show clearly for all three orientations studied and are particularly clear for the 90° orientation, where the amplitude of the Fourier peak is larger than that of the peak at 3.3 Å. However, the authors do not include any discussion of these peaks at distances shorter than 1.89 Å. The feature at 3.3 Å is attributed to Mn backscattering, but the peak at 3.8 Å is unexplained. An asymmetric cluster containing four Mn atoms is proposed, with Mn - Mn distances of 2.7 Å and 3.3 Å.

Some possible reasons for the discrepancies in the reports of features at about 1.8 Å and at greater than 3.0 Å between our recent data and those of George *et al* are: 1) Differences in the preparation procedures; we have utilized fully active PS II particles in our study. The data of George *et al* are based on chloroplast membranes. In our experience chloroplast membranes are labile with respect to Mn release; the procedure and time required to orient samples make it possible that some of the Mn was dislodged in the process. The lack of a Mn(II) EPR signal does not insure that Mn(II) is not dislodged, because bound Mn(II) frequently does not give rise to the

familiar six-line EPR signal. Although the Mn K-edge position is not specified in the paper, it appears in the figure that the inflection point is at less than 6550 eV, which suggests that Mn may have been released as Mn(II). 2) The data collections are carried out at different temperatures. 3) The use of empirical phase shift and amplitude functions in their study (from $KMnO_4$ for the Mn-O parameters and from the adamantane-like cluster for Mn-Mn parameters) can lead to misleading results especially when applied to structures which are unknown. Transferability of phase shift and amplitude functions works best when the structures are as similar chemically as possible.[50b,c] The O environment in $KMnO_4$, or the Mn environment in the adamantane-like cluster, is not typical of what one finds in oxo-bridged Mn complexes with Mn-Mn distances of 2.7 Å.

Structural Changes During S-State Transitions. The Fourier transforms of the EXAFS data from the S_1, S_2 and S_3 states in Fig 4 show that the Fourier peaks are similar for the three states. Detailed EXAFS fitting shows that the structure of the Mn complex in the O_2-evolving complex remains substantially unchanged during the $S_1 \rightarrow S_2$ and $S_2 \rightarrow S_3$ transitions.

The EXAFS spectra from the S_1 and S_2 preparations are indistinguishable; the main features at 1.75 - 1.8, 1.9 - 2.2 and ~2.7 Å are invariant not only for the dark S_1 state and 190 K-illuminated S_2 state, but also for the S_2 state prepared at 277 K, where ligand exchange might occur.[39] Similar results were derived from spinach and from *Synechococcus* preparations.[21b] We conclude that, although the S_1 to S_2 transition involves a change in the oxidation state as discussed earlier, there is no EXAFS-detectable change in the oxo-bridged complex of Mn. The similarity of the results from spinach and *Synechococcus* in the S_1 and S_2 states is suggestive that the structure of the Mn complex is largely conserved across the evolutionary diversity of O_2-evolving photosynthetic species.

The S_3 state is also not markedly different from the S_2 state in terms of the coordination environment of Mn.[42] Detailed comparison of the Mn EXAFS with model compounds indicates that there are subtle differences between the S_2 and S_3 states which are best explained in terms of an increase in the spread of Mn-Mn distances. The simplest explanation is that there are two very similar di-μ-oxo bridged structures in the S_2 state, while in the S_3 state the Mn-Mn distances differ by ~ 0.15 Å.

The lack of a significant change of the EXAFS of Mn in the S_2 to S_3 transitions argues strongly against recent proposals by Brudvig *et al* [59] that a significant structural rearrangement

from a cubane-like to an adamantane-like tetranuclear Mn structure occurs at this transition. The EXAFS spectrum of a tetranuclear adamantane-like Mn complex synthesized by Wieghardt *et al* [54d] with a Mn-Mn distance of 3.2 Å is very different from the spectrum of the OEC in the S_3 state (or those of the S_0^*, S_1 or S_2 states). This excludes adamantane-like structures as relevant models for the Mn cluster in the S_0^* through S_3 states states. Each Mn atom in cubane-like or adamantane-like structures is linked by three bridging O atoms at about 1.8Å. Simulations of EXAFS data from PS II samples show that the number of scatterers at about 1.8Å from Mn is less than two, which constitutes additional evidence against these tetranuclear structures.

Christou and Vincent[60] have proposed two interesting mechanisms of O_2 evolution based on multinuclear Mn complexes synthesized by their group. Both mechanisms involve major structural rearrangements in the $S_1 \rightarrow S_2$, and/or the $S_2 \rightarrow S_3$ transition, where an "open butterfly-like" structure is transformed into a distorted cubane-like structure. The EXAFS data exclude such major changes in the structure of the complex in the $S_1 \rightarrow S_2$ and $S_2 \rightarrow S_3$ transitions for the photosynthetically derived preparations.

A peroxo-bridged structure was suggested for either the S_2 or the S_3 state,[61] on the basis that two-electron oxidation of water to form a peroxo compound is favored thermodynamically over sequential one-electron oxidations. It is unlikely that the Mn atoms which are separated by 2.7 Å are bridged by peroxo moieties in S_1, S_2 or S_3, because peroxo bridged structures are characterized by a longer Mn-Mn distance.[13a] Such bridges might occur *between* two binuclear clusters, however.

The EXAFS spectrum of the S_0^* state is significantly different from that of the S_1 state.[41] An examination of the Fourier transforms shows that there is a significant decrease in the amplitude of the Fourier peaks in the S_0^* state relative to the S_1 state (Fig 7). Detailed EXAFS analysis indicates that the oxo-bridged Mn structure is present in S_0^*, but there is a larger spread of Mn-Mn and Mn-ligand atom distances in the S_0^* state compared to that in the S_1 state. An examination of the Fourier transforms from tetranuclear complexes with similar ligands but in different oxidation states, (II,III,III,III) and (III,III,III,III), reveals a similar decrease in the amplitudes of the Fourier peaks in the complexes with mixed-valence structure containing Mn(II) (Fig 7). The decrease in amplitude is a reflection of the larger spread (0.1 to 0.15 Å) in Mn-Mn

distances and in Mn -O or -N ligand distances present in mixed-valence inorganic complexes containing Mn(II). The K-edge position and the EXAFS spectrum of the Mn complex in the S_0^* state are indicative of a heterogeneous mixture of formal valences of Mn, including one Mn(II) which is not present in the S_1 state.

Mn Oxidation and Water Splitting

The relation between the accumulation of oxidizing equivalents by the Mn complex and the reactions by which water is deprotonated, the O-O bond is formed and O_2 is released remains to be determined. Renger[61] proposed that the role of the Mn complex is to stabilize reactive intermediates like hydroxyl radicals that would otherwise react irreversibly and destructively with the photosynthetic membrane components. Brudvig and Crabtree[59] proposed a mechanism in which a rearrangement of an adamantane-like Mn complex led to the formation of the O-O bond. Christou and Vincent[60] described a molecular "double pivot" mechanism to accomplish the same objectives. These models make the implicit assumption that Mn is somehow directly involved in the water splitting and O_2 formation. There is no experimental evidence that this is the case, however.

The EXAFS results indicate that there are no major changes in the oxo-bridged structure of the Mn complex in the S_0^* through S_3 states. The X-ray K-edge data indicate that the oxidation state of the Mn complex increases by one equivalent during the S_0^* to S_1 and also during the S_1 to S_2 transitions. No similar change is seen upon the S_2 to S_3 transition; however, a change in the magnetics of the system does occur, reflected by the loss of the S_2 EPR multiline signal in S_3.

These results from spectroscopic studies raise some interesting possibilities for the mechanism of water oxidation and O_2 evolution in PS II preparations from plants and cyanobacteria. 1) *The Mn complex is involved in the storage of oxidizing equivalents, but the actual oxidation of water may occur at some other site.* A recent report by Plijter, *et al.*[62] adds significant new evidence to the case for the separation of Mn oxidation and water splitting. This is based on their observation that there is a significant delay (30 to 130ms) between the advance of the Mn complex beyond the S_3 state and the appearance of O_2 at a polarographic electrode. This surprising conclusion, which is in contradiction to long-standing reports in the literature by Joliot, *et al.*[63] and confirmed by others,[64] results in large part from refining the polarographic conditions

used previously for measuring O_2 evolution and that were inappropriate for determination of the kinetics. Not only is the release of O_2 from the water-splitting enzyme slow, but during the interval of about 100ms awaiting the release of O_2 the Mn complex can continue to be advanced in the S-state cycle all the way to the next S_3 state. At that point the release from the enzyme of the product O_2 from the previous turn of the cycle must occur before further S-state advance is possible. A straightforward explanation for this behavior proposed by Plijter, *et al* [62] is that the accumulation of oxidizing equivalents by the Mn complex is separate and distinct from the conversion of water to O_2. 2) *The oxidation of water to O_2 is a concerted reaction occurring during the S_3 to S_0 transition,* a transition which has not been studied by XAS. In fact, several experiments point to the possibility that the Mn complex accumulates the oxidizing equivalents by simple electron transfer steps, to reach S_3, and that the oxidation of water occurs in a concerted reaction that then leaves the Mn complex in its most reduced state, S_0. One such proposal is based on mass spectrometric experiments indicating that the involvement of water does not occur until after the S_3 state has been reached.[65] Another finding that is consistent with this view is that the advance from S_1 to S_2 to S_3 involves very little, if any, structural change in the Mn complex, based on the EXAFS evidence discussed above. If one of the mechanisms proposed by Brudvig and Crabtree[59] or by Christou and Vincent[60] was applicable, we would expect to see a major change in the linkage between Mn and its coordinating ligands during the S_2 to S_3 transition, when significant molecular rearrangements were proposed to occur. The studies of Guiles, *et al*,[42] however, found no evidence for such a structural change in the vicinity of the Mn. 3) *It is possible to oxidize water without invoking major changes in the oxo-bridging structure of the Mn complex.* For example the oxidation could be occurring between two di-μ-oxo bridged moieties, which are separated by greater than 3 Å. No such mechanism has been described at a detailed structural level yet, but it is entirely feasible that the chemistry involving the formation of the O-O linkage and subsequent release of O_2 occurs between the two binuclear Mn clusters. This would explain the invariance of the core structure seen by X-ray spectroscopy. The formation of the O-O linkage is the crucial step in the oxidation of water, and attempts to rationalize the formation of this linkage have led to various mechanistic proposals[59,60] that invoke major changes in the Mn core structure. The formation of the peroxo bond (O-O), which is a prerequisite for O_2 formation, has not yet been demonstrated by any spectroscopic method.

An important implication of the results of Plijter, *et al*[62] described above is that the site of accumulation of oxidizing equivalents (the Mn complex) and the site of water-splitting and O_2 formation may be functionally separate. The process could still involve the concerted transfer of 4

electrons following activation of the S_3 state, but the O_2 precursor thus formed may require further rearrangement (time) before O_2 is released. During this interval the redox active part of the Mn complex is able to continue to store oxidizing equivalents up to the next S_3 state. It remains to be determined the extent to which the sites of oxidant accumulation and of O_2 formation are *physically* separate from one another. Clearly this is an important area for research that will attract much attention in the near future.

Acknowledgements

We wish to acknowledge with appreciation the contributions of Mn model compounds provided by Prof. G. Christou (Indiana University, Bloomington), Prof. K. Wieghardt (Ruhr University, Bochum, FRG and Prof. W. H. Armstrong (University of California, Berkeley) and their research groups. Vickie DeRose provided original spectra as well as helpful comments on the manuscript. The research originating from our laboratory and described in this overview was supported, in part, by the Director, Office of Energy Research, Office of Basic Energy Sciences, Biological Energy Research Division of the U.S. Department of Energy under Contract No. DE-AC03-76SF00098, by a grant from the U.S. Department of Agriculture (85-CRCR-1-1847) and by a grant from the National Science Foundation (DMB88-04526).

References

(1) (a) Joliot, P.; Barbieri, G.; Chabaud, R. *Photochem. Photobiol.* **1969**, *10*, 309-329. (b) Kok, B.; Forbush, B.; McGloin, M. *Photochem. Photobiol.* **1970**, *11*, 457-475.

(2) Pirson, A. *Z. Botan.* **1937**, *31*, 193-267.

(3) Yamashita, T.; Butler, W. L. *Plant Physiol.* **1968**, *43*, 1978-1986; **1969**, *44*, 435-438.

(4) Yamashita, T.; Tsuji, J.; Tomita, G. *Plant Cell Physiol.* **1971**, *12*, 117-126.

(5) (a) Blankenship, R. E.; Sauer, K. *Biochim. Biophys. Acta* **1974**, *357*, 252-266; (b) Blankenship, R. E.; Babcock, G. T.; Sauer, K. *Biochim. Biophys. Acta* **1975**, *387*, 165-175.

(6) Radmer, R.; Cheniae, G.M. *Top. Photosynth.* **1977**, *2*, 303-348.

(7) (a) Fowler, C.F. *Biochim. Biophys. Acta* **1977**, *459*, 351-363; **1977**, *462*, 414-421. (b) Saphon, S.; Crofts, A. R. *Z. Naturforsch. C: Biosci.* **1977**, *32C*, 617-626.

(8) (a) Amesz, J. *Biochim. Biophys. Acta* **1983**, *726*, 1-12. (b) Babcock, G.T. In *New Comprehensive Biochemistry*, vol. 15. *Photosynthesis*; Amesz, J., Ed.; Elsevier: Amsterdam, 1987; pp 125-158. (c) Andréasson, L.-E., Vänngård, T. *Ann. Rev. Plant Physiol. Plant Mol. Biol.* **1988**, *39*, 379-411.

(9) (a) Dismukes, G. C.; Siderer, Y. *FEBS Lett*. **1980**, *121*, 78-80. (b) Dismukes, G. C.; Siderer, Y. *Proc. Natl. Acad. Sci. USA* **1981**, *78*, 274-278.

(10) Hansson, Ö.; Andréasson, L.-E. *Biochim. Biophys. Acta* **1982**, *697*, 261-268.

(11) Brudvig, G. W.; Casey, J. L.; Sauer, K. *Biochim. Biophys. Acta* **1983**, *723*, 366-371.

(12) Cooper, S. R.; Dismukes, G. C.; Klein, M. P.; Calvin, M. *J. Am. Chem. Soc.* **1978**, *100*, 7248-7252.

(13) (a) Mabad, B.; Tuchagues, J.-P.; Hwang, Y. T.; Hendrickson, D. N. *J. Am. Chem. Soc.* **1985**, *107*, 2801-2802. (b) Chang, H.-R.; Diril, H.; Nilges, M. J.; Zhang, X.; Potenza, J. A.; Schugar, H. J;.Hendrickson, D. N.; Isied, S.S. *J. Am. Chem. Soc.* **1988**, *110*, 625-627. (c) Chang, H.-R.; Larsen, S. K.; Boyd, P. D. W.; Pierpont, C. G.; Hendrickson, D. N. *J. Am. Chem. Soc.* **1988**, *110*, 4565-4576.

(14) Hansson, Ö.; Aasa, R.; Vänngård, T. *Biophys. J.* **1987**, *51*, 825-832.

(15) (a) Dismukes, G. C.; Ferris, K.; Watnick, P. *Photobiochem. Photobiophys.* **1982**, *3*, 243-256. (b) de Paula, J. C.; Beck, W. F.; Brudvig, G. W. *J. Am. Chem. Soc.* **1986**, *108*, 4002-4009.

(16) Fronko, R. M.; Penner-Hahn, J. E.; Bender, C. J. *J. Am. Chem. Soc.* **1988**, *110*, 7554-7555.

(17) (a) Yachandra, V. K.; Guiles, R. D.; Sauer, K.; Klein, M. P. *Biochim. Biophys. Acta* **1986**, *850*, 333-342. (b) Nugent, J. H. A. *Biochim. Biophys. Acta,* **1987**, *893*, 184-189.

(18) (a) Casey, J. L.; Sauer, K. *Biochim. Biophys. Acta* **1984**, *767*, 21-28. (b) Zimmermann, J.-L.; Rutherford, A. W. *Biochim. Biophys. Acta* **1984**, *767*, 160-167.

(19) Zimmermann, J.-L.; Rutherford, A. W. *Biochem.* **1986**, *25*, 4609-4615.

(20) Cole, J.; Yachandra, V. K.; Guiles, R. D.; McDermott, A. E.; Britt, R. D.; Dexheimer, S. L.; Sauer, K.; Klein, M. P. *Biochim. Biophys. Acta* **1987**, *890*, 395-398.

(21) (a) Aasa, R.; Andréasson, L.-E.; Lagenfelt, G.; Vänngård, T. *FEBS Lett.* **1987**, *221*, 245-248. (b) McDermott, A. E.; Yachandra, V. K.; Guiles, R. D.; Cole, J. L.; Dexheimer, S. L.; Britt, R. D.; Sauer, K.; Klein, M. P. *Biochem.* **1988**, *27*, 4021-4031.

(22) Singer, L. S. *J. Chem. Phys.* **1955**, *23*, 379-388.

(23) (a) Richens, D. T.; Sawyer, D. T. *J. Am. Chem. Soc.* **1979**, *101*, 3681-3683. (b) Magers, K. D.; Smith, C. G.; Sawyer, D. T. *Inorg. Chem.* **1980**, *19*, 492-496.

(24) Lindahl, P. A.; Day, E. P.; Kent, T. A.; Orme-Johnson, W. H.; Münck, E. *J. Biol. Chem.* **1985**, *260*, 11160-11173.

(25) Maki, A. H.; McGarvey, B. R. *J. Chem. Phys.* **1958**, 29, 35-38.

(26) (a) Mims, W. B. In *Electron Paramagnetic Resonance*; Geschwind, S., Ed.; Plenum Press: New York, 1972; pp 263-351. (b) Kevan, L. (1979) In *Time Domain Electron Spin Resonance*; Kevan, L.; Schwartz, R.; Eds.; Wiley: New York, 1979; pp 279-341. (c) Mims, W. B.; Peisach, J. In *Biological Magnetic Resonance*; Berliner, L. J.; Reuben, J.; Eds.; Plenum Press: New York, 1981; Vol 3, pp 213-263. (d) Thomann, H.; Dalton, L. R.; Dalton, L. A. In *Biological Magnetic Resonance*; Berliner, L. J.; Reuben, J.; Eds.; Plenum Press: New York, 1984; Vol 6, pp 143-186.

(27) Britt, R. D.; DeRose, V. J.; Chan, M.; Armstrong, W. H.; Sauer, K.; Klein, M. P. (submitted to *J. Am. Chem. Soc.*)

(28) Britt, R. D.; Zimmermann, J.-L.; Sauer, K.; Klein, M. P. *J. Am. Chem. Soc.* **1989**, *111*, 3522-3532.

(29) (a) Sandusky, P. O.; Yocum, C. F. *Biochim. Biophys. Acta* **1984**, *766*, 603-611. (b) Sandusky, P. O.; Yocum, C. F. *Biochim. Biophys. Acta* **1986**, *849*, 85-93.

(30) Beck, W. F.; de Paula, J. C.; Brudvig, G. W. *J. Am. Chem. Soc.* **1986**, *108*, 4018-4022.

(31) Boussac, A.; Rutherford, A. W. *Biochem.* **1988**, *27*, 3476-3483.

(32) Powers, L. *Biochim. Biophys. Acta* **1982**, *683*, 1-38.

(33) Sayers, D. E.; Stern, E. A.; Lytle, F. W. *Phys. Rev. Lett.* **1971**, *27*, 1204-1207.

(34) (a) Kuwabara, T.; Murata, N. *Plant Cell Physiol.* **1982,** *23*, 533-539. (b) Satoh, K.; Ohno, T.; Katoh, S. *FEBS Lett.* **1985,** *180*, 326-330.

(35) Shulman, R. G.; Yafet, Y.; Eisenberger, P.; Blumberg, W. E. *Proc. Natl. Acad. Sci. USA* **1976**, *73*, 1384-1388.

(36) Kutzler, F. W.; Natoli, C. R.; Misemer, D. K.; Doniach, S.; Hodgson, K.O. *J. Chem. Phys.* **1980**, *73*, 3274-3288.

(37) (a) Kirby, J. A.; Goodin, D. B.; Wydrzynski, T.; Robertson, A. C.; Klein, M. P. *J. Am. Chem. Soc.* **1981,** *103*, 5537-5542. (b) Cramer, S. P.; Eccles, T. K.; Kutzler, F.W.; Hodgson, K. O.; Mortenson, L. E. *J. Am. Chem. Soc.* **1976,** *98*, 1287-1288.

(38) Goodin, D. B.; Yachandra, V. K.; Britt, R. D.; Sauer, K.; Klein, M. P. *Biochim. Biophys. Acta* **1984,** *767*, 209-216.

(39) Yachandra, V. K.; Guiles, R. D.; McDermott, A. E.; Cole, J. L.; Britt, R. D.; Dexheimer, S. L.; Sauer, K.; Klein, M. P. *Biochem.* **1987,** *26*, 5974-5981.

(40) (a) Cartier, C.; Verdaguer, M.; Menage, S.; Girerd, J.-J.; Tuchagues, J. P.; Mabad, B. *Journal de Physique C8*, **1986**, 623-625. (b) Yachandra, V. K.; Guiles, R. D., unpublished results.

(41) Guiles, R. D.; Yachandra, V. K.; McDermott, A. E.; Cole, J. L.; Dexheimer, S. L.; Britt, R. D.; Sauer, K.; Klein, M.P. (1989) *Biochem.* **1989** in press.

(42) Guiles, R. D.; Zimmermann, J.-L.; McDermott, A. E.; Yachandra, V. K.; Cole, J. L.; Dexheimer, S. L.; Britt, R. D.; Wieghardt, K.; Bossek, U.; Sauer, K.; Klein, M.P. *Biochem.* **1989** in press.

(43) Sauer, K.; Guiles, R. D.; McDermott, A. E.; Cole , J. L.; Yachandra, V. K.; Zimmermann, J.-L.; Klein, M. P.; Dexheimer, S. L.; Britt, R. D. *Chemica Scripta* **1988,** *28A*, 87-91.

(44) (a) Dekker, J. P.; Van Gorkom, H. J.; Brok, M.; Ouwehand, L. *Biochim. Biophys. Acta* **1984**, 764, 301-309. (b) Saygin, Ö.; Witt, H. T. *Biochim. Biophys. Acta* **1987,** *893*, 452-469.

(45) (a) Srinivasan, A.N.; Sharp, R.R. *Biochim. Biophys Acta* **1986,** *851*, 369-376. (b) Evelo, R.G.; Styring, S.; Rutherford, A.W.; Hoff, A.J. *Biochim. Biophys. Acta* **1989** *973*, 428-442.

(46) Kretschmann, H.; Dekker, J. P.; Saygin, Ö.; Witt, H. T. *Biochim. Biophys. Acta* **1988,** *932*, 358-361.

(47) Vincent, J. B.; Christou, G. *FEBS Lett.* **1986,** *207*, 250-252.

(48) McDermott, A. E.; Yachandra, V. K.; Guiles, R. D.; Britt, R. D.; Dexheimer, S. L.; Sauer, K.; Klein, M. P. *Biochem.* **1988,** *27*, 4013-4020.

(49) Kambara, T.; Govindjee *Proc. Natl. Acad. Sci. USA* **1985** *82*, 6119-6123.

(50) (a) Teo, B.-K.; Lee, P. A. *J. Am. Chem. Soc.* **1979**, *101*, 2815-2832. (b) Teo, B.-K.; Antonio, M.R.; Averill, B.A. *J. Am. Chem. Soc.* **1983**, *105*,3751-3762. (c) Teo, B.-K. EXAFS: *Basic Principles and Data Analysis*; Springer Verlag: New York, 1986.

(51) George, G. N.; Prince, R. C.; Cramer, S. P. *Science* **1989**, *243*, 789-791.

(52) (a) Plaksin, P. M.; Stoufer, R. C.; Mathew, M.; Palenik, G. J. *J. Am. Chem. Soc.* **1972**, *94*, 2121-2122. (b) Stebler, M.; Ludi, A.; Bürgi, H.-B. *Inorg. Chem.* **1986**, *25*, 4743-4750. (c) Wieghardt, K.; Bossek, U.; Zsolnai, L.; Huttner, G.; Blondin, G.; Girerd, J.-J.; Babonneau, F. *J. Chem. Soc., Chem. Commun.* **1987**, 651-653. (d) Wieghardt, K.; Bossek, U.; Nuber, B.; Weiss, J.; Bonvoisin, J.; Corbella, M.; Vitols, S. E.; Girerd, J.-J. *J. Am. Chem. Soc.* **1988**, *110*, 7398-7411.

(53) (a) Vincent, J. B.; Christmas, C.; Huffman, J. C.; Christou, G.; Chang, H.-R.; Hendrickson, D.N. *J. Chem. Soc., Chem. Commun.* **1987**, 236-238. (b) Christmas, C.; Vincent, J. B.; Huffman, J. C.; Christou, G.; Chang, H.-R.; Hendrickson, D. N. *J. Chem. Soc., Chem. Commun.* **1987**, 1303-1305. (c) Bashkin, J. S.; Chang, H.-R.; Streib, W. E.; Huffman, J. C.; Hendrickson, D. N.; Christou, G. *J. Am. Chem. Soc.* **1987**, *109*, 6502-6504.

(54) (a) Wieghardt, K.; Bossek, U.; Ventur, D.; Weiss, J. *J. Chem. Soc., Chem. Commun.* **1985**, 347-349. (b) Sheats, J. E.; Czernuszewicz, R. S.; Dismukes, G. C.; Rheingold, A. L.; Petrouleas, V.; Stubbe, J.; Armstrong, W. H.; Beer, R. H.; Lippard, S. J. *J. Am. Chem. Soc.* **1987**, *109*, 1435-1444. (c) Wieghardt, K.; Bossek., U.; Bonvoisin, J.; Beauvillain, P.; Girerd, J.-J.; Nuber, B.; Weiss, J.; Heinze, J. *Angew. Chem.* **1986**, *98*, 1026-1027. (d) Wieghardt, K.; Bossek, U.; Gebert, W. *Angew. Chem.* **1983**, *95*, 320.

(55) Guiles, R.D.; Yachandra, V.K.; McDermott, A.E.; Britt, R.D.; Dexheimer, S.L.; Sauer, K.; Klein, M.P. In *Progress in Photosynthesis Research*; Biggins, J., Ed.; Nijhoff: Dordrecht, 1987; vol. 1, pp 561-564.

(56) Goulding, F. S.; Landis, D. A.; Madden, N. W. *IEEE Trans. Nucl. Sci.* **1983**, *30*, 301-310.

(57) Powers, L.; Chance, B.; Ching, Y.; Angiolillo, P. *Biophys. J.* **1981**, *34*, 465-498.

(58) (a) Li, X.; Kessissoglou, D.P.; Kirk, M.L.; Bender, C.J.; Pecoraro, V.L. *Inorg. Chem.* **1988**, *27*, 1-3. (b) Kessissoglou, D.P.; Lah, M.S.; Pecoraro, V.L. *Angew. Chem.* **1989**, submitted.

(59) Brudvig, G. W.; Crabtree, R. H. *Proc. Natl. Acad. Sci. USA* **1986**, *83*, 4586-4588.

(60) Christou, G.; Vincent, J. B. *Biochim. Biophys. Acta* **1987**, *895*, 259-274.

(61) Renger, G. In *Photosynthetic Oxygen Evolution*; Metzner, H., Ed.; Academic: London, 1978; pp 229-248.

(62) Plijter, J.J.; Aalbers, S.E.; Barends, J.-P.; Vos, M.H.; van Gorkom, H.J. *Biochim. Biophys. Acta* **1988**, *935*, 299-311.

(63) Joliot, P.; Hofnung, M.; Chabaud, R. *J. Chim. Phys.* **1966**, *63*, 1423-1441.

(64) (a) Sinclair, J.; Arnason, T. *Biochim. Biophys. Acta* **1974**, *368*, 393-400. (b) Arnason, T.; Sinclair, J. *Biochim. Biophys. Acta* **1976**, *430*, 517-523. (c) Etienne, A. L. *Biochim. Biophys. Acta* **1968**, *153*, 895-897.

(65) (a) Radmer, R.; Ollinger, O. *FEBS Lett.* **1986**, *195*, 285-289. (b) Bader, K.P.; Thibault, P.; Schmidt, G.H. *Biochim. Biophys. Acta* **1987**, *893*, 564-571.

Table I

a) Mn Complexes with Similar Structures and in Different Oxidation States	Mn K-edge Inflection Point Energy (eV)	Δ (eV)
1) Mn_2 (III,III) (μ_2-O) (μ_2-Ac)$_2$ (tmtacn)$_2$ (ClO_4)$_2$ Mn_2 (III,IV) (μ_2-O) (μ_2-Ac)$_2$ (tacn)$_2$ (ClO_4)$_3$	6549.6 6550.5	0.9
2) Mn_2(III,IV) (μ_2-O)$_2$ (Phen)$_4$ (PF_6)$_3$ Mn_2 (IV,IV) (μ_2-O)$_2$ (Phen)$_4$ (ClO_4)$_4$	6550.1 6551.9	1.8
3) Mn_3 (II,III,III) (μ_3-O) (μ_2-Bz)$_6$ (Py)$_2$ (H_2O) Mn_3 (III,III,III) (μ_3-O) (μ_2-Bz)$_6$ (Im)$_3$ (ClO_4)$_2$ [NBu_4]	6549.3 6550.9	1.6
4) Mn_3 (II,III,III) (μ_3-O) (μ_2-Ac)$_6$ (Py)$_3$·Py Mn_3 (III,III,III) (μ_3-O) (μ_2-Ac)$_6$ (Py)$_3$ (ClO_4)	6548.8 6550.7	1.9
5) Mn_4 (II,III,III,III) (μ_3-O)$_2$ (μ_2-Bz)$_7$ (bipy)$_2$ Mn_4 (III,III,III,III) (μ_3-O)$_2$ (μ_2-Bz)$_7$ (bipy)$_2$ (ClO_4)	6548.6 6550.6	2.0
b) Mn Complexes with Different Structures and in in Similar Oxidation States		
1) Mn_2 (III,IV) (μ_2-O) (μ_2-Ac)$_2$ (tacn)$_2$ (ClO_4)$_3$ Mn_2(III,IV) (μ_2-O)$_2$ (Phen)$_4$ (PF_6)$_3$	6550.5 6550.1	0.4
2) Mn_2 (III,IV) (μ_2-O) (μ_2-Ac)$_2$ (tacn)$_2$ (ClO_4)$_3$ Mn_2 (III,IV) (μ_2-O)$_2$ (bipy)$_4$ (ClO_4)$_3$	6550.5 6549.9	0.6

where

Ac = acetate; tmtacn=N',N",N"-trimethyl-1,4,7-triazacyclononane;

tacn = 1,4,7-triazacyclononane; Phen = 1,10-Phenanthroline; Bz = benzoate; Py = pyridine;

Im = Imidazole; NBu_4 = tetra-N-butylammonium ion; bipy = 2,2'-bipyridine

Table II

S- State	Schemes for Oxidation State Changes			
	a	b	c	d
S_0	II,III,III,III	II,III,IV,IV	III,III,III,IV	II,II,III,IV
S_1	III,III,III,III	III,III,IV,IV	III,III,IV,IV	II,III,III,IV
S_2	III,III,III,IV	III,IV,IV,IV	III,IV,IV,IV	III,III,III,IV
S_3	III,III,III,IV	III,IV,IV,IV	III,IV,IV,IV	III,III,III,IV

The oxidation states of manganese listed under a and b are in better agreement with XAS data than those listed under c and d, and, therefore, may be more likely.

Figure Captions

Figure 1 EPR signals associated with the oxygen evolving center in spinach PS II preparations: (a) The multiline EPR signal formed by advancement to the S_2 state following continuous illumination at 195 K. Frequency, 9.2 GHz; temperature, 8 K; power, 30mW; modulation amplitude, 32 G. (b) The g=4.1 EPR signal produced by continuous illumination of a sample at 170 K in the presence of 0.4 M sucrose. Frequency, 9.2 GHz; temperature, 10 K; power, 50mW; modulation amplitude, 32 G. The displayed EPR spectra result from the subtraction of background EPR spectra recorded prior to illumination. (These spectra were kindly provided by V. J. DeRose and J. L. Cole.)

Figure 2. The continuous-wave EPR spectrum for the mixed valence binuclear Mn complex di-μ-oxo-tetrakis(2,2'-bipyridine)dimanganese(III,IV) perchlorate with the ^{15}N isotope of nitrogen incorporated into the 2,2'-bipyridine ligands. Frequency, 9.2 GHz; temperature, 8 K; power, 1mW; modulation amplitude, 1.0 G. (Figure adapted from reference 27.) The compound was synthesized by Michael Chan and Prof. W. H. Armstrong (University of California, Berkeley).

Figure 3 Cosine Fourier transforms of the ESEEM patterns obtained for PSII membrane preparations following 195 K illumination and subsequent warming to 20 °C for 30 s. (a) Two-pulse ESEEM spectrum for control sample with no added NH_4Cl. The peak at 15 MHz arises from weakly coupled protons. The origin of the low frequency peak in the control sample is under investigation. (b) Two-pulse ESEEM spectrum for the sample treated with $^{15}NH_4Cl$. The new peak at 3 MHz arises from an ammonia-derived ^{15}N ligand to the Mn complex. (c) Two-pulse ESEEM spectrum for the sample treated with $^{14}NH_4Cl$. Additional modulation is observed at 4.5 MHz, along with several lower frequency transitions. (d) Three-pulse ESEEM spectrum for the sample treated with $^{14}NH_4Cl$. The low frequency transitions resolved in the three-pulse data correspond to the "zero-field" transitions for the ammonia-derived ^{14}N ligand, with quadrupolar coupling values of $eeqQ$=1.61 MHz and η=0.59. The ESEEM data were all obtained at temperature, 4.2 K; microwave excitation frequency, 9.2446 GHz; magnetic field, 3500 G; time interval between spin echo pulse sets, 4.0 ms. (Figure adapted from reference 28).

Figure 4 Fourier transforms of the k^1-weighted Mn EXAFS data of spinach PS II samples in the S_1, S_2 and S_3 states. The first peak is primarily due to bridging O (or N) ligands at ~1.8 Å and terminal O (or N) ligands at 1.9-2.2 Å. The second peak is primarily due to Mn at ~2.7 Å. These peaks are characteristic of a di-μ-oxo-bridged Mn cluster. The peaks appear at an apparent distance R', which is shorter than the real internuclear distance. Note the similarity of the Fourier transforms in the S_1, S_2 and S_3 states.

Figure 5 Different bridging structures and the respective Mn-Mn distances: (a) A pair of Mn atoms linked by a di-μ_2-oxo bridge. Typical Mn-Mn distances in synthetic complexes with such a structure is ~2.7 Å.[52] (b) An additional μ_2-acetate bridge does not change the Mn-Mn distance significantly. The Mn-Mn distance is 2.6 Å in a complex with a di-μ_2-oxo linkage,[52c] and ~2.8 Å in complexes with di-μ_3-oxo linkages.[53a,b] (c) In complexes with two μ_2-acetate bridges and one μ_2-oxo bridge the Mn-Mn distance is between 3.1-3.2 Å.[54a-c] (d) Pairs of Mn atoms are linked by a single μ_2-oxo bridge in the adamantane-like complex and the Mn-Mn distance is 3.2 Å.[54d] (e) In the 'butterfly' tetranuclear complex, the Mn- Mn distance between the Mn atoms linked by the two μ_3-oxo bridges is ~2.8 Å.[53a,b] There is also an additional acetate bridge. The distance between the 'wing tip' and the central Mn atom is between 3.3-3.5 Å.

Figure 6 A model for the Mn complex in the OEC. The simplest interpretation of the EXAFS data is that there are two di-μ-oxo bridged Mn clusters separated by greater than 3 Å. The Mn-Mn distance in each of the di-μ-oxo bridged clusters is ~2.7Å.

Figure 7 (a) Fourier transforms of the k^1-weighted Mn EXAFS of an S_1 state preparation (_____) and S_0^* state preparation (- - - -). The significantly lower amplitude of the S_0^* state

Fourier transform indicates a more disordered system, with a larger spread in Mn-O, N and Mn-Mn distances. The distances R' in the Fourier transforms are shorter than the true bond lengths. (b) The Fourier transforms of the k^1-weighted Mn EXAFS of a tetranuclear Mn complex Mn_4 (III,III,III,III) $(\mu_3\text{-O})_2$ $(\mu_2\text{-Bz})_7$ $(\text{bipy})_2$ (ClO_4) is shown as the solid trace. The dashed line is the Fourier transform of an isostructural manganese tetranuclear complex Mn_4 (II,III,III,III) $(\mu_3\text{-O})_2$ $(\mu_2\text{-Bz})_7$ $(\text{bipy})_2$ which contains one Mn(II) ion not present in the former isostructural complex. Note the reduction in the amplitude of the Fourier peaks is remarkably similar to that observed between the S_1 and S_0^* states.

"Multiline" EPR Signal

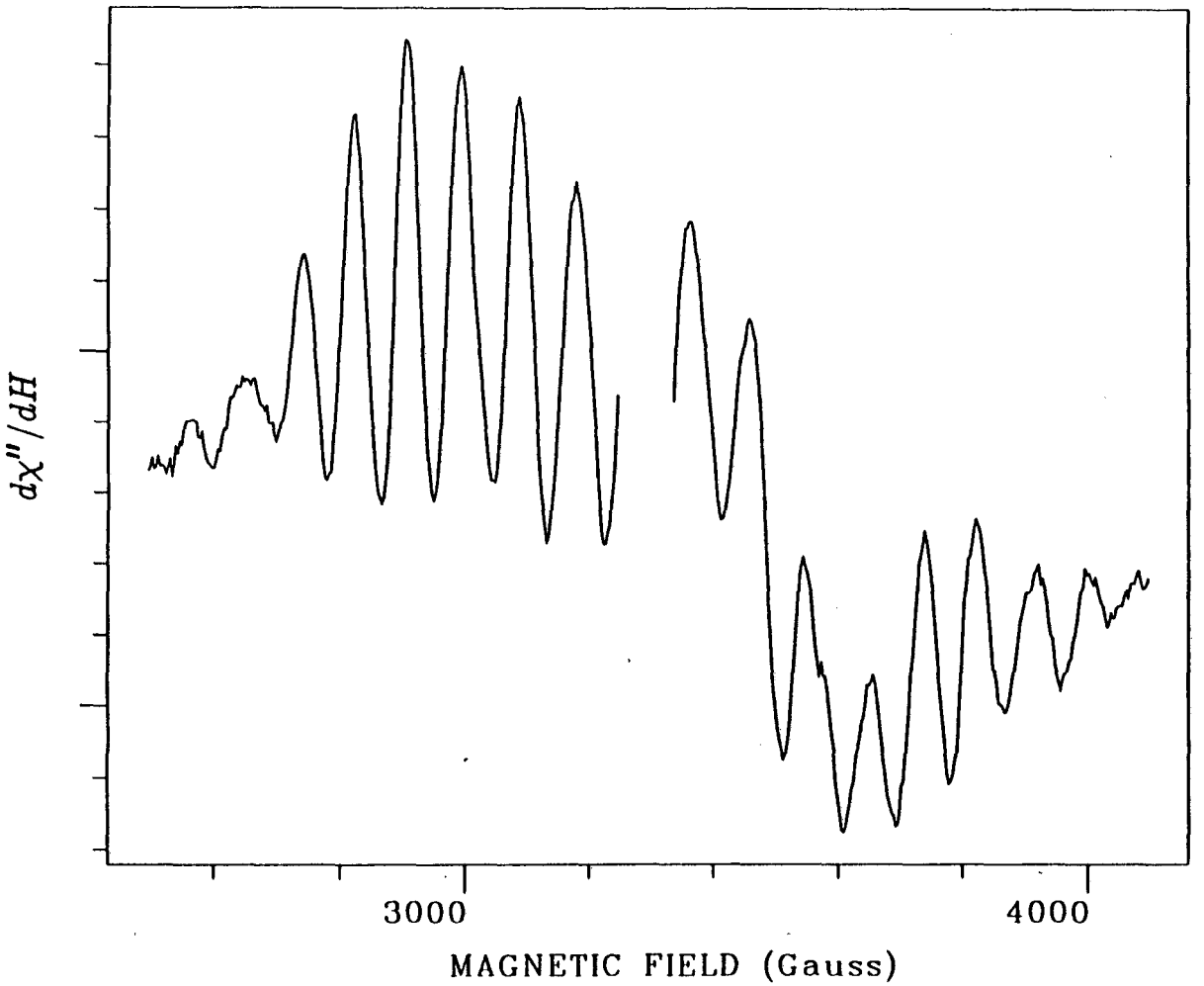

XBL 895-1957

Sauer et al.

Fig. 1a

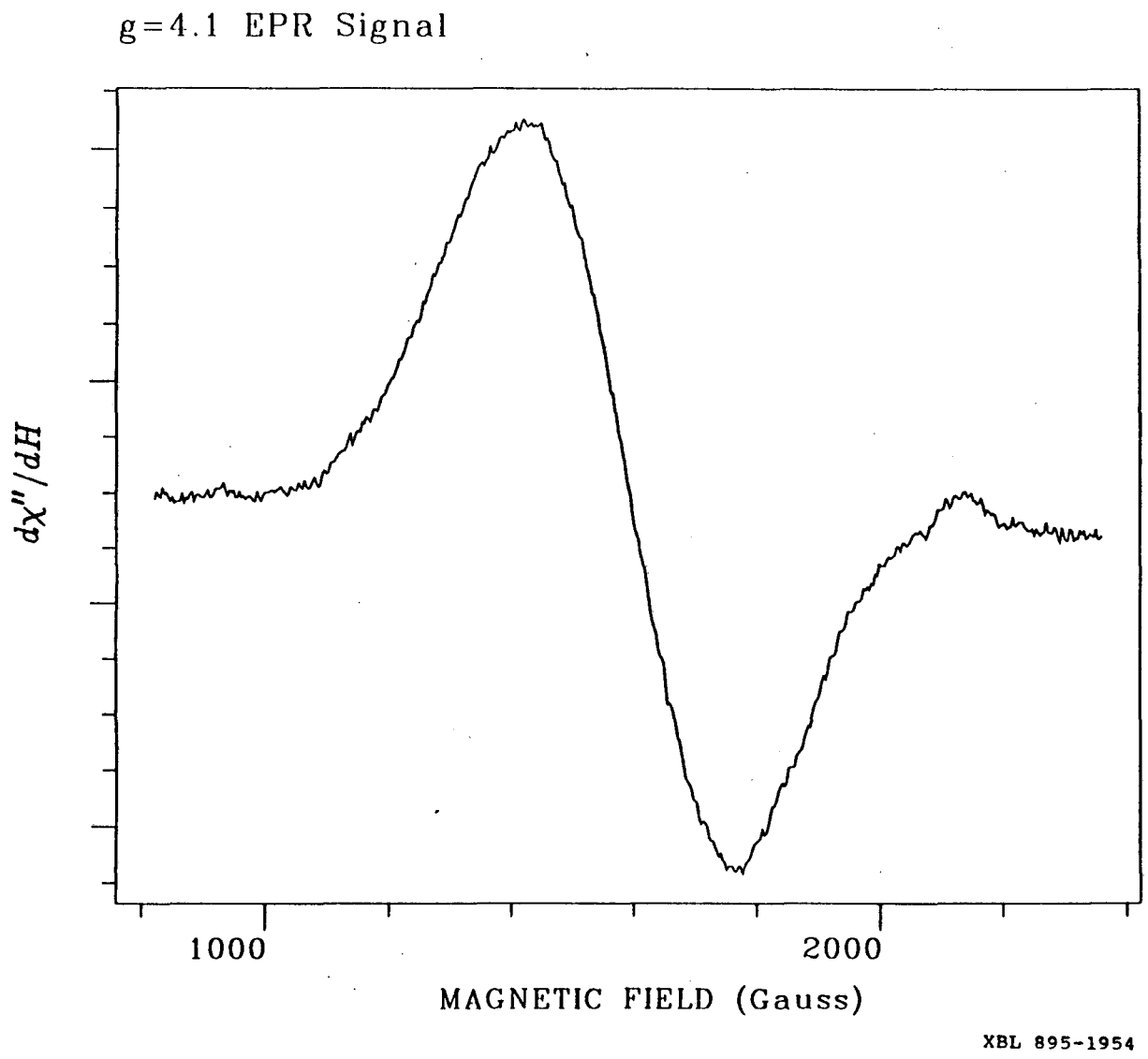

Sauer et al.

Fig. 1b

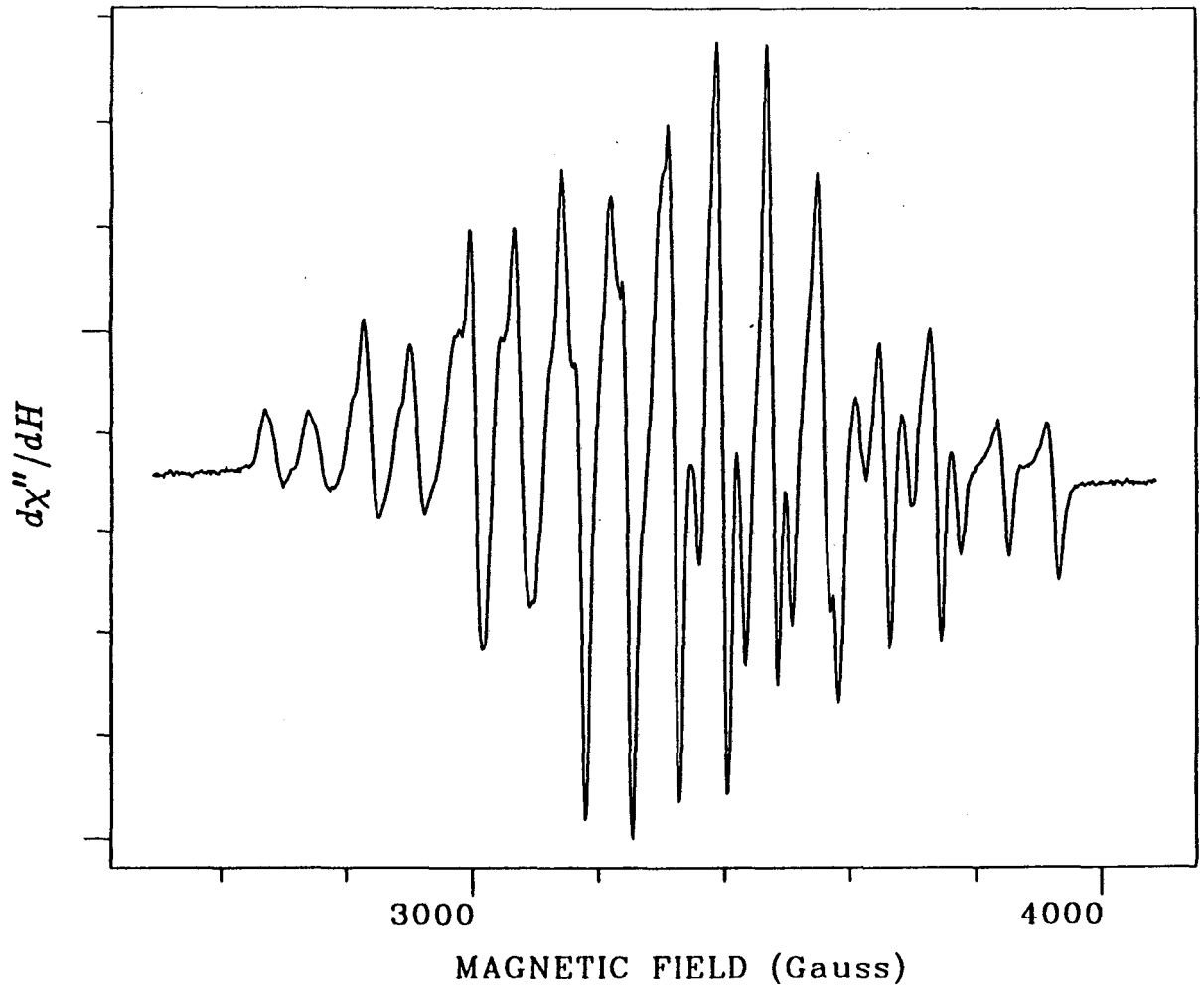

XBL 895-1953

Sauer et al.

Fig. 2

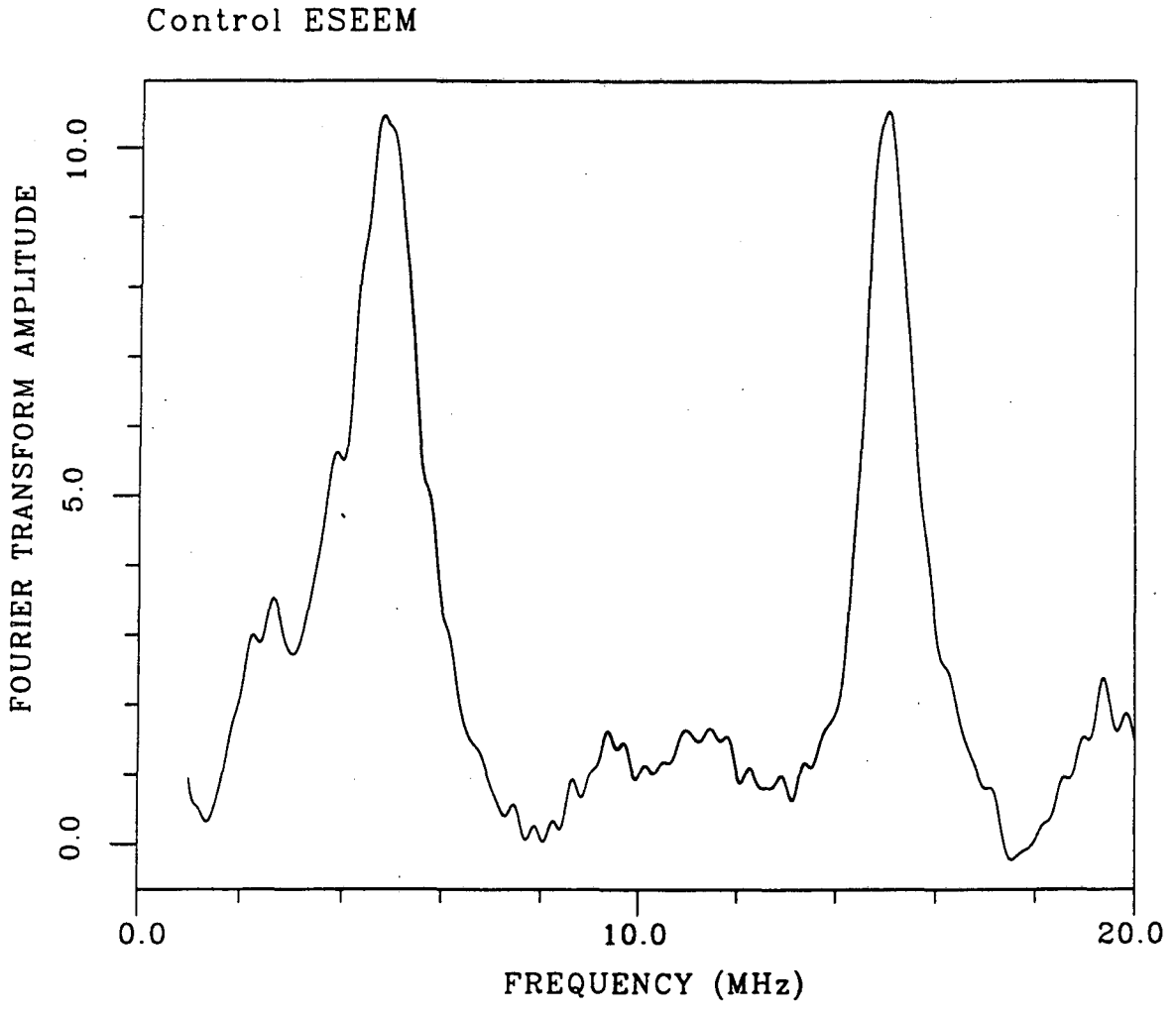

XBL 895-2035

Sauer et. al

Fig. 3a

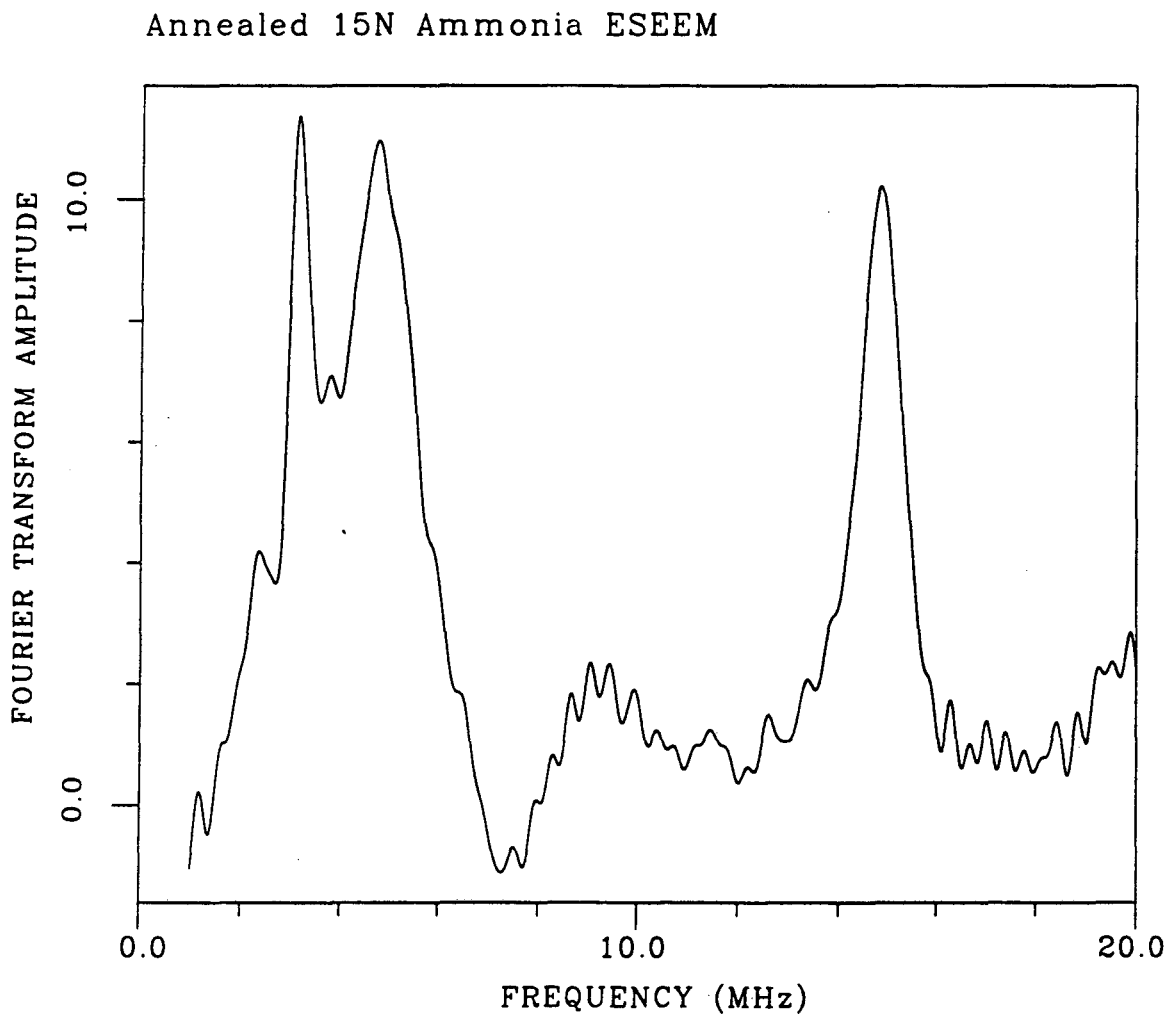

XBL 895-2036

Sauer et al.

Fig. 3b

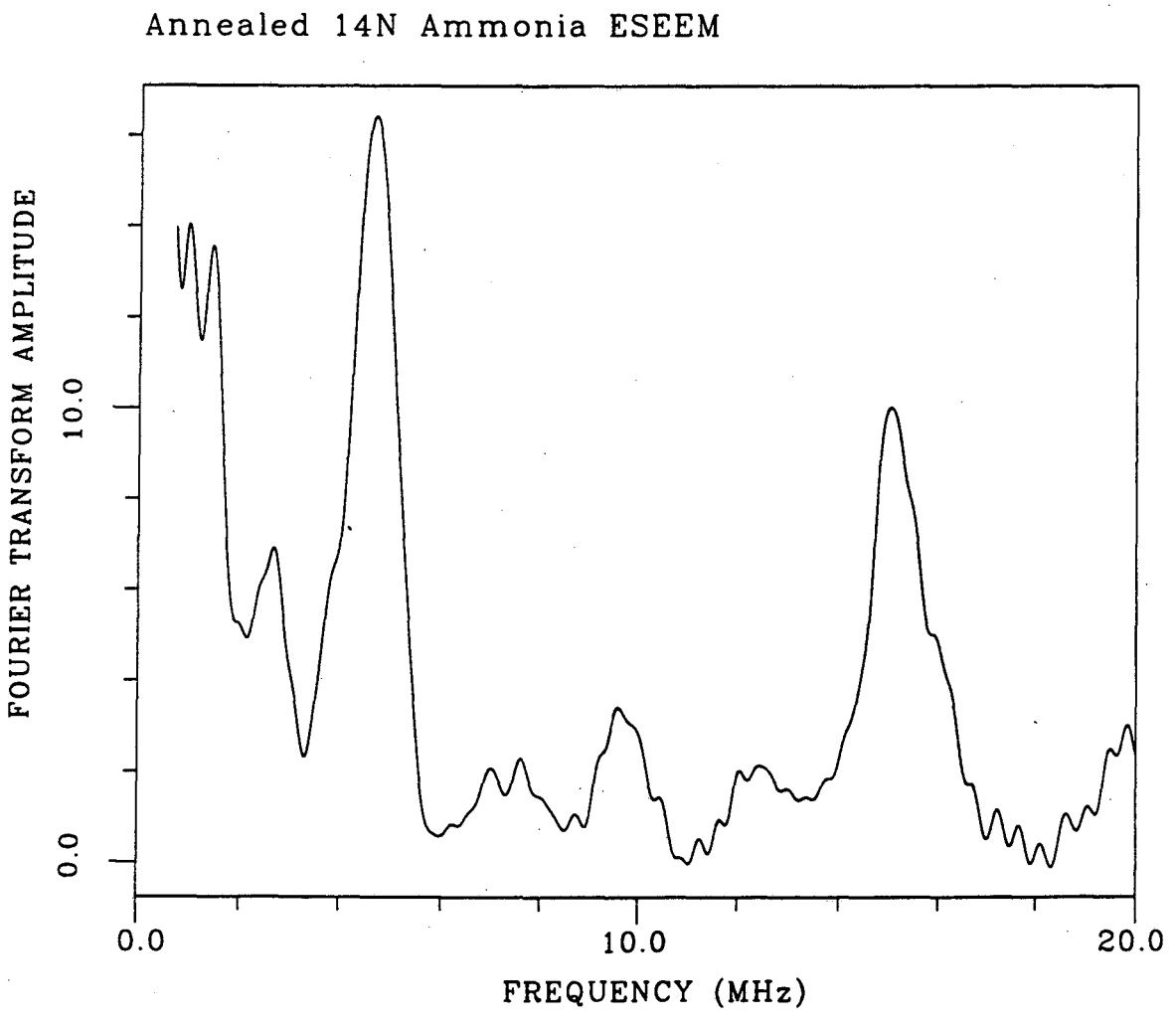

XBL 895-2034

Sauer et al.

Fig. 3c

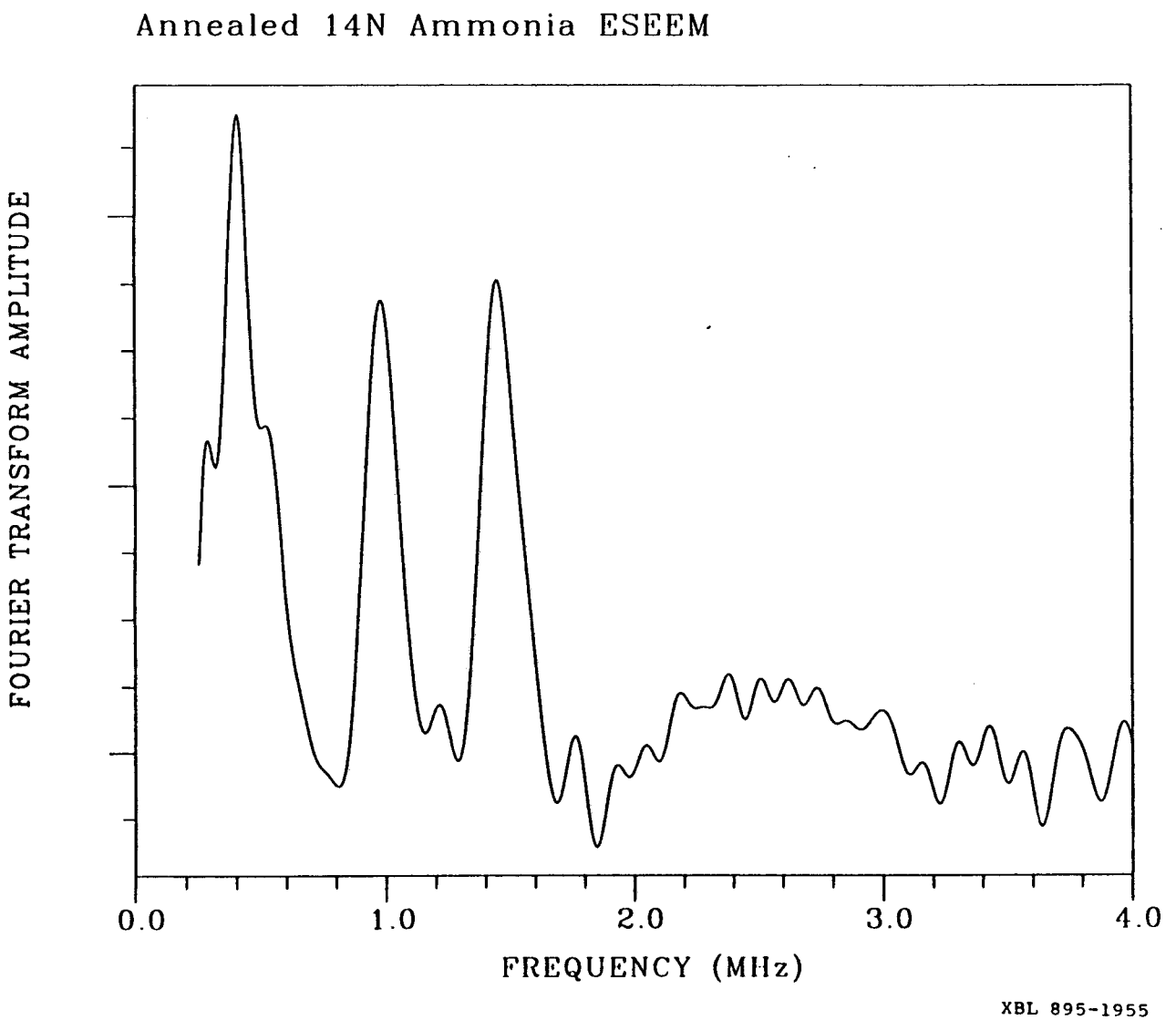

Sauer et al.

Fig. 3d

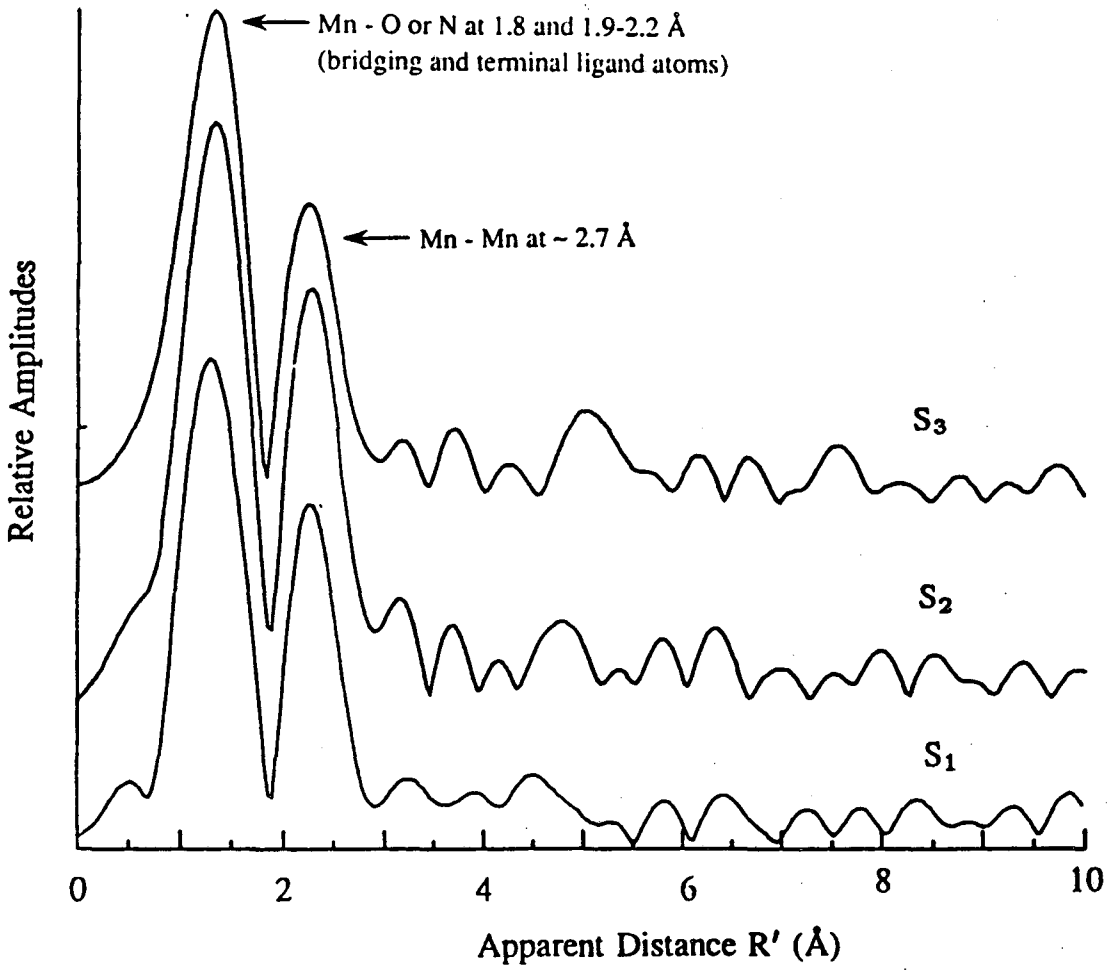

XBL 895-1778

Sauer et al.

Fig. 4

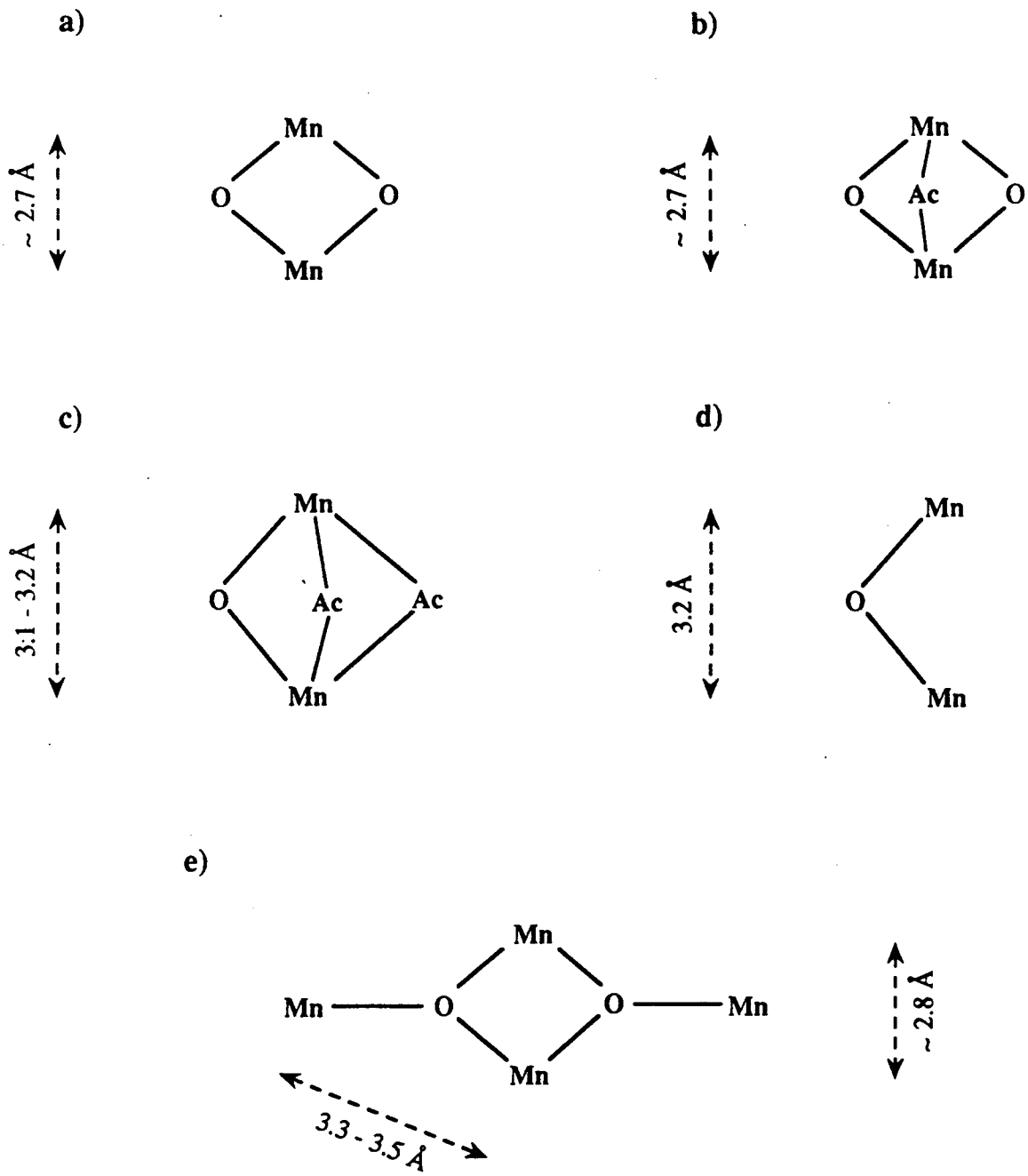

XBL 895-1777

Sauer et al.

Fig. 5

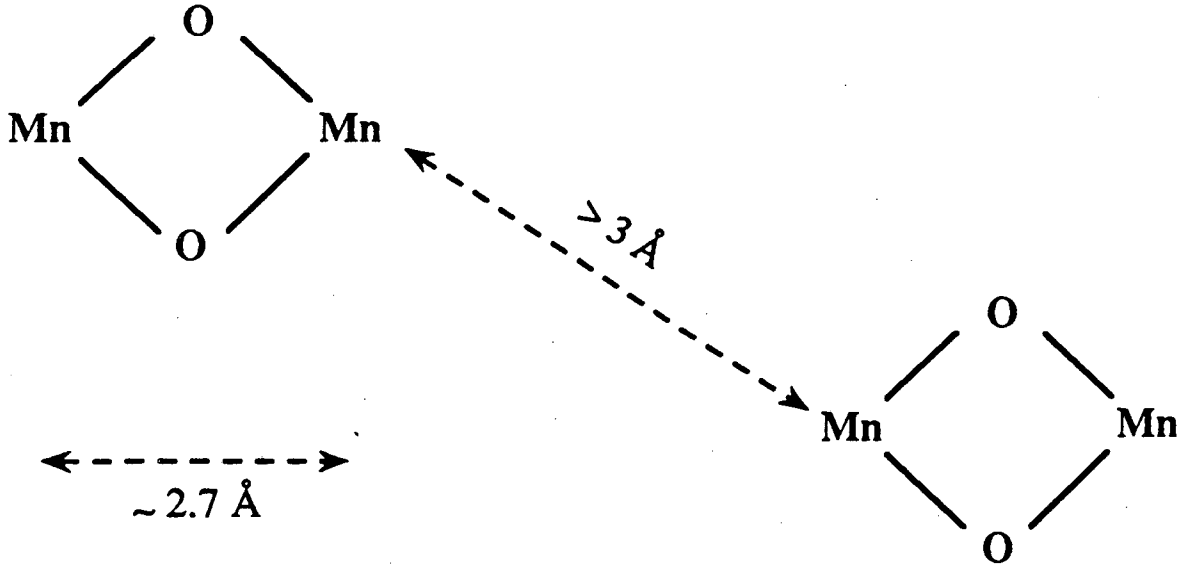

XBL 895-1776

Sauer et al.

Fig. 6

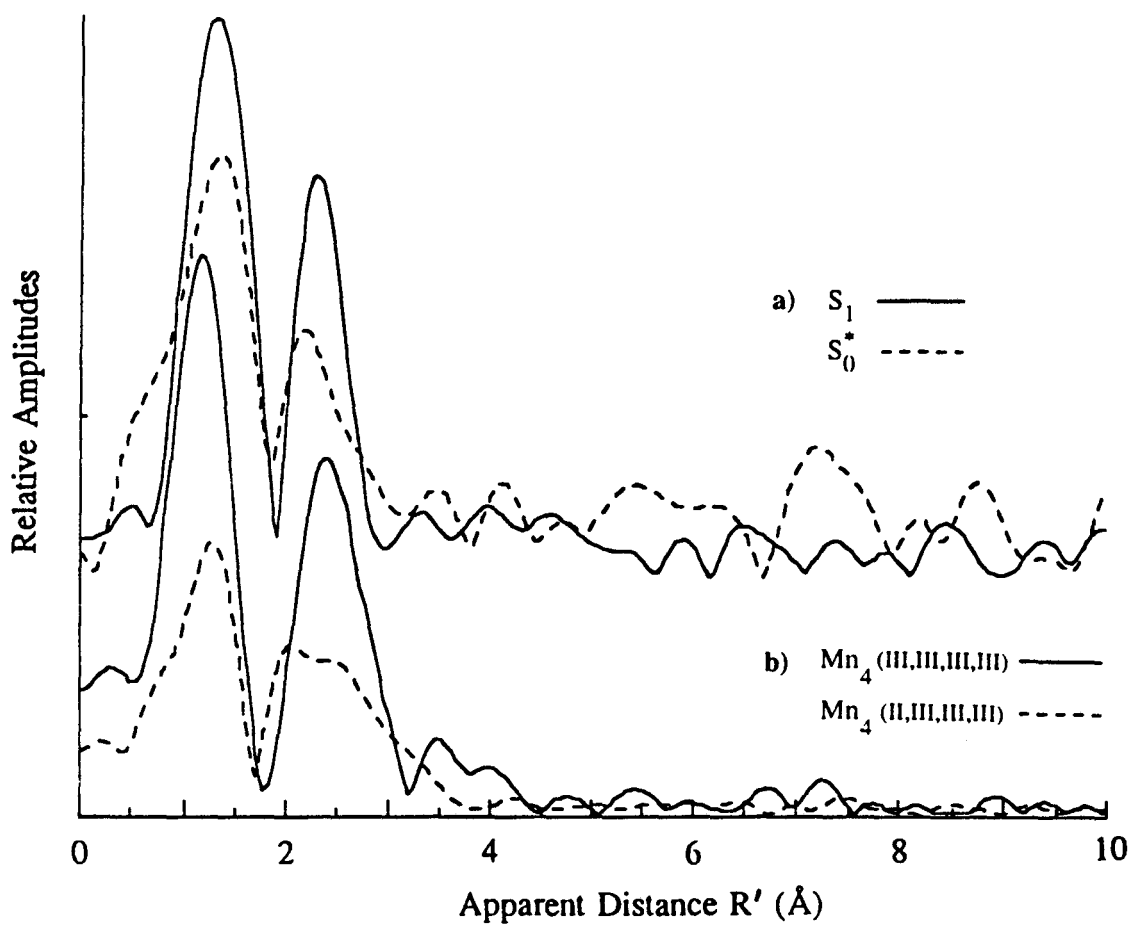

XBL 895-1779

Sauer et al.

Fig. 7

LAWRENCE BERKELEY LABORATORY
TECHNICAL INFORMATION DEPARTMENT
UNIVERSITY OF CALIFORNIA
BERKELEY, CALIFORNIA 94720